NASA/TM–2015-218681

Comparison of Flight Simulators Based on Human Motion Perception Metrics

Ana R. Valente Pais and Bruno J. Correia Grácio
Delft University of Technology, Delft, The Netherlands

Lon C. Kelly
Unisys Corporation, Hampton, Virginia

Jacob A. Houck
Langley Research Center, Hampton, Virginia

February 2015

NASA STI Program . . . in Profile

Since its founding, NASA has been dedicated to the advancement of aeronautics and space science. The NASA scientific and technical information (STI) program plays a key part in helping NASA maintain this important role.

The NASA STI program operates under the auspices of the Agency Chief Information Officer. It collects, organizes, provides for archiving, and disseminates NASA's STI. The NASA STI program provides access to the NTRS Registered and its public interface, the NASA Technical Reports Server, thus providing one of the largest collections of aeronautical and space science STI in the world. Results are published in both non-NASA channels and by NASA in the NASA STI Report Series, which includes the following report types:

- TECHNICAL PUBLICATION. Reports of completed research or a major significant phase of research that present the results of NASA Programs and include extensive data or theoretical analysis. Includes compilations of significant scientific and technical data and information deemed to be of continuing reference value. NASA counter-part of peer-reviewed formal professional papers but has less stringent limitations on manuscript length and extent of graphic presentations.

- TECHNICAL MEMORANDUM. Scientific and technical findings that are preliminary or of specialized interest, e.g., quick release reports, working papers, and bibliographies that contain minimal annotation. Does not contain extensive analysis.

- CONTRACTOR REPORT. Scientific and technical findings by NASA-sponsored contractors and grantees.

- CONFERENCE PUBLICATION. Collected papers from scientific and technical conferences, symposia, seminars, or other meetings sponsored or co-sponsored by NASA.

- SPECIAL PUBLICATION. Scientific, technical, or historical information from NASA programs, projects, and missions, often concerned with subjects having substantial public interest.

- TECHNICAL TRANSLATION. English-language translations of foreign scientific and technical material pertinent to NASA's mission.

Specialized services also include organizing and publishing research results, distributing specialized research announcements and feeds, providing information desk and personal search support, and enabling data exchange services.

For more information about the NASA STI program, see the following:

- Access the NASA STI program home page at http://www.sti.nasa.gov

- E-mail your question to help@sti.nasa.gov

- Phone the NASA STI Information Desk at 757-864-9658

- Write to:
  NASA STI Information Desk
  Mail Stop 148
  NASA Langley Research Center
  Hampton, VA 23681-2199

Comparison of Flight Simulators Based on Human Motion Perception Metrics

Ana R. Valente Pais and Bruno J. Correia Grácio
Delft University of Technology, Delft, The Netherlands

Lon C. Kelly
Unisys Corporation, Hampton, Virginia

Jacob A. Houck
Langley Research Center, Hampton, Virginia

Abstract

In flight simulation, motion filters are used to transform aircraft motion into simulator motion. When looking for the best match between visual and inertial amplitude in a simulator, researchers have found that there is a range of inertial amplitudes, rather than a single inertial value, that is perceived by subjects as optimal. This zone, hereafter referred to as the optimal zone, seems to correlate to the perceptual coherence zones measured in flight simulators. However, no studies were found in which these two zones were compared. This study investigates the relation between the optimal and the coherence zone measurements within and between different simulators. Results show that for the sway axis, the optimal zone lies within the lower part of the coherence zone. In addition, it was found that, whereas the width of the coherence zone depends on the visual amplitude and frequency, the width of the optimal zone remains constant.

Contents

1 Introduction

Ideally, flight simulators would expose pilots to visual and inertial cues indistinguishable from those experienced during real flight. However, the visual and inertial cues in the simulator have limitations not encountered during real flight. For example, visual cues are limited by the projection system (e.g., resolution, luminance, contrast), transport delay, low spatial frequency, and no stereoscopic cues. Nonetheless, the visual amplitude can be reproduced one-to-one in most flight simulators. The inertial cues, however, have to be scaled down to guarantee that the simulator is kept within its physical limits.

The use of motion filters ensures that the mechanical limits of the simulator are not reached while providing inertial cues to the pilots. These motion filters introduce amplitude and phase distortions with respect to the real aircraft motion and to the displayed visual cues.

To guarantee a high fidelity of the simulation, the impact of these differences on the pilot has to be understood. Throughout the years, many studies have, therefore, focused on understanding pilot perception in simulator environments [1–13] and others have investigated the effect of motion cues and motion filter settings on pilot behavior [14–19]. There also has been some effort in categorizing different filter settings in equivalent fidelity regions [20–23].

Some studies have focused specifically on the combined perception of visual and inertial stimuli [24–26]. It has been shown in various driving simulation [27, 28] and flight simulation studies [6, 29] that simulations where the visual and inertial cues had equal magnitudes were not preferred by subjects. In these studies, the amplitude of the inertial cues was lowered because subjects perceived the inertial motion as "too strong".

This overestimation of inertial motion was hypothesized to occur due to the differences between the simulator and real world visual properties [29], and due to motion distortions imposed by the motion filters and the vehicle model [30]. Regardless of the reason for the overestimation, it is clear that using current simulation technology, a one-to-one match between inertial and visual cues may not be the best choice. Inertial motion amplitudes different from the visual motion amplitudes may still be acceptable or even better than the one-to-one case.

For a better understanding of which amplitudes of inertial motion are perceived as acceptable, or even optimal, in a simulation environment, two approaches have been developed: the measurement of perception coherence zones (CZ) [31–34], and the measurement of optimal zones (OZ) [35].

The CZ is a concept first introduced by Van der Steen [31, 32] when studying amplitude differences between visual and inertial cues. He defined the CZ as a zone where inertial and visual amplitudes are perceived to be coherent although their amplitudes are different. To obtain a CZ,

the maximum and minimum inertial amplitudes that are still perceived as coherent with a certain visual amplitude are measured. These maximum and minimum coherent amplitudes are referred to as the upper and lower thresholds, respectively.

More recently the work of Van der Steen has been extended to include different types of stimuli, such as higher amplitudes [34] and different frequencies [33], to investigate the effect of workload on CZ [36] and to measure not only amplitude coherence zones but also phase coherence zones [37].

Amplitude coherence zones are influenced by a number of factors such as the amplitude and frequency [33, 34, 38] of the visual stimuli. Coherence zones seem to also be significantly affected by the type of visual and motion system used. In ValentePais *et al.* [33], data from two different simulators were compared and it was observed that the measured coherence zones were different between simulators. Such a result indicates that when transforming coherence zone knowledge to motion filter design and tuning, attention should be given to the simulator specific configuration in terms of motion base and visual system.

The OZ was introduced in a study by Correia Grácio *et al.* [35]. Using sinusoidal signals as stimuli, they asked their subjects to tune the inertial motion amplitude such that it would optimally match the amplitude of the presented visual scene motion. Although researchers expected to find a single inertial amplitude matching the visual amplitude, results showed that the optimal inertial amplitude depended on the initial value of the inertial amplitude. When the amplitude of the inertial motion of their first run was well above the amplitude of the visual stimulus, subjects tended to choose higher optimal gains than when having a first run with a lower inertial amplitude. As a consequence, the optimal gain value became an optimal gain zone, delimited by the higher and lower values found.

From this result, the question arose to whether the measured optimal zone was not in fact a coherence zone. Moreover, it was thought that whether or not these zones are equivalent, they might be useful in the tuning of motion filters for specific simulator configurations. For this purpose it is necessary to test how much of the differences among simulators can be captured by coherence zones, optimal zones, or both.

To investigate what was the relationship between optimal zone and coherence zone, and whether these two metrics could indeed differentiate between simulator configurations, a study was designed where optimal gain measurements and coherence zone measurements in sway were made using the same subjects, stimuli and identical measurement methods in three different simulators [39].

An experiment was conducted at the NASA Langley Research Center in Hampton, Virginia, where both the Cockpit Motion Facility (CMF) and the Visual Motion Simulator (VMS) were used. In the CMF two

different cockpits were used: the Generic Flight Deck (GFD) and the Integration Flight Deck (IFD). In all three simulators, the OZ and the CZ were measured. Both zones were measured for two different stimulus amplitudes and two different frequencies. The measurements were performed in sway, so that the results can be compared to previous studies [27, 28, 35].

This report will discuss the results of the experiment and is structured as follows. In Section 2 we will briefly discuss the concepts and earlier results obtained regarding the coherence and optimal zone experiments. Section 3 describes the experimental method used, the results are given in Section 4 and discussed in detail in Section 5. The report ends with conclusions and recommendations for future work.

2 Background

2.1 Coherence Zone

When humans walk or control a vehicle, the visual information is coherent with the inertial information. To detect self-motion, the human body integrates information from the visual, vestibular, and somatosensory systems, and combines it with the expectation derived from bodily actions. In the real world, the visual information is always matched to the vestibular information one-to-one. However, this might not be the case in a simulation environment, where the visual information can be completely different from the inertial information. For example, a simulator visual could be displaying a 10 meter movement while the motion base only moved 1 meter.

If the difference between the visual and inertial information is too large, humans will detect that the perceived inertial movement is incongruent with the visual scene. To study these types of visual-inertial interactions, Van der Steen [31, 32] introduced the concept of coherence zone (CZ). The CZ defines a perceptual zone where the visual and inertial cues are perceived as "coherent". In this paper, the coherence zones are studied in terms of amplitude differences between visual and inertial cues. However, the concept of CZ can also be extended to include other stimulus properties such as phase differences [26, 37].

To define a CZ, one needs to measure the maximum and minimum inertial amplitudes that are still considered by subjects to be coherent with a particular visual amplitude. The maximum coherent amplitude is defined as the upper threshold (th_{up}), whereas the minimum coherent amplitude is defined as the lower threshold (th_{lo}). To capture the CZ, the coherence zone width (CZW) and the point of mean coherence (PMC) metrics can be defined using Equations (1) and (2), respectively.

$$CZW = th_{up} - th_{lo} \qquad (1)$$

$$PMC = th_{lo} + \frac{CZW}{2} \qquad (2)$$

In Ref. [34], three experiments are described that aimed at extending the knowledge on the CZs first measured by Van der Steen [32]. In the first experiment, the CZ measured by Van der Steen [32] was extended to higher amplitudes. The CZs were measured for visual amplitudes of 0, 4, 12, 18, 22, 26, and 30 deg/s^2. The motion profile used for the visual and inertial motion was based on smoothed steps in acceleration. An up-down staircase procedure was used to obtain both the upper and lower thresholds. Subjects had to answer affirmatively or negatively the following question: "Did the amplitude of the visual movement correspond with the magnitude of the motion?". Then, using a staircase algorithm, the inertial motion of the next run would change, while the visual motion would remain constant. Based on the subjects' successive answers, the inertial motion would then converge to a certain value, later used to calculate the upper and lower thresholds.

Results showed that, up to a visual amplitude of 12 deg/s^2, the obtained CZs were very similar to the ones measured by Van der Steen [32]. The PMC showed values close to the corresponding visual amplitudes while the CZW increased with the visual amplitude. However, for higher visual amplitudes the PMCs became smaller than the corresponding visual amplitudes; the CZW remained approximately constant with the increase of the visual amplitude.

In a second experiment, the staircase measurement method was compared with a self-tuning method where subjects could decide the amount of inertial motion they would like to experience in the next run. This was done because the staircase method was time consuming and the task proved to be difficult for the subjects. Details on the latter self-tuning method are discussed in Subsection 3.4 of this report. Using the two methods, the CZ was measured for the 12 and 30 deg/s^2 amplitudes. The motion profiles were again based on smoothed steps in acceleration. For both the PMC and CZW measurements, the results obtained with the two measurement methods were very similar, and the small differences in the data obtained with both methods were not statistically significant. This does not mean, however, that both methods are equal and that their use would always yield the same results. Since the experiments presented in this paper are very similar to those with which the measurement methods yielded similar data, we were confident however that in this particular case the self-tuning method would lead to the same trends as the more task-demanding staircase method. It is recommended to study the wider validity of this claim in later experiments.

In a third experiment, the effect of the frequency of the motion stimulus on the CZ was tested. The chosen visual amplitudes were again 12 and 30 deg/s^2. In this experiment there were three different motion profiles: a sinusoid with a frequency of 2 rad/s, a sinusoid with a fre-

quency of 10 rad/s, and the smoothed step in acceleration used in the previous experiments. The self-tuning method was used to measure the CZs. Results showed that the PMC as well as the CZW increase with the stimulus amplitude (similar to the first experiment) but decreased with the stimulus frequency. The frequency dependency of the results was hypothesized to be related to the dynamics of the semicircular-canals [34].

2.2 Optimal Zone

In theory, one-to-one simulation (i.e., when inertial cues are equal to visual cues) should result in the best perceived match between visual and inertial information. However, recent studies have shown that one-to-one motion in a simulation can be perceived as too strong [6, 27–29]. In driving simulation, Feenstra et al. [27] studied the effect of providing drivers with different motion conditions during a slalom maneuver. They tested motion gains, the ratio between inertial and visual motion, of 0, 0.4, 0.7, and 1. A motion gain of 0 means that only visual information was displayed while a motion gain of 1 means that the visual information corresponded to the inertial information. Surprisingly, results showed that 0.7 was the preferred motion gain. The Motion Cueing Algorithm (MCA) used in this experiment cued the lateral road position one-to-one. However, longitudinal specific force was not cued because the car travelled at constant speed. All the other degrees-of-freedom (DoF) where cued one-to-one. In all DoFs a limiter block was used to prevent damage of the simulator whenever the actuators were close to their limits. Pretto et al. [28] conducted a similar study in a different simulator. The authors stated that in this experiment, the vehicle dynamics from the simulated car were directly mapped to the simulator motion. The motion system had a transport delay of 41ms. They tested motion gains of 0.5, 0.75, 1, and 1.25. Results showed that the value 0.5 and 0.75 were most preferred by subjects. Similar trends in the motion gain were also found in flight simulation. Groen et al. [6] tested different motion filter configurations to simulate a take off maneuver. The preferred motion filter conditions involved a motion gain of 0.2 for the surge filter and a motion gain of 0.6 for the pitch filter. Groen et al. [6] stated in the study that, "Remarkably, unity gains were rejected as [being] too powerful." However, in this study the MCA cued high-frequency longitudinal cues with simulator surge and low-frequency longitudinal cues with simulator pitch (tilt-coordination). This classical way of cueing might have introduced distortions in the motion profiles [30]. In another study, pilots reported that the lateral motion experienced during a decrab maneuver was too strong, even though the motion gain was 0.7 [29]. According to the authors, in this condition the motion from the aircraft model was sent directly to the motion platform without involving any MCA in the process. The visual delay was about 50 ms.

To determine if these reported motion gains were being influenced

by the vehicle model, an experiment where subjects were asked to find the "best match" between the visual and inertial amplitude was conducted [35]. This best match is hereafter referred to as Optimal Zone (OZ). The OZ was measured in sway for sinusoidal motion profiles in acceleration with amplitudes of 1 and 2.5 m/s^2 and frequencies of 0.2, 0.4 and 0.8 Hz. Subjects were given a visual stimulus with constant amplitude and were asked to change the inertial amplitude until they decided that the 'best match' between the visual and inertial acceleration was obtained. A side-stick was used to change the inertial amplitude while experiencing the constant visual amplitude. A left-deflection reduced the inertial amplitude while a right deflection increased it. At the start of a measurement, an initial inertial amplitude was provided that was either higher or lower than the corresponding visual amplitude. Results showed that this initial inertial amplitude influenced the optimal zone. An initial inertial amplitude set higher than a certain visual amplitude led to inertial amplitudes that were higher than those obtained when the initial inertial amplitude was set lower than the same visual amplitude. As a result, each visual amplitude had two values where the inertial motion was perceived to be 'optimal', thus resulting in an optimal *zone*. The upper boundary of the optimal zone is referred to as the upper optimal amplitude; the lower boundary of the optimal zone is referred to as the lower optimal amplitude.

In the same study it was found that the inertial amplitude chosen by subjects decreased for stimuli with higher frequency, suggesting a sensitivity to the acceleration derivative (i.e., jerk) as reported in previous research [30, 40, 41]. There was also an effect of the visual signal amplitude. The visual signal with an amplitude of 2.5 m/s^2 led to lower motion gains than the conditions using a visual signal with an amplitude of 1 m/s^2.

When comparing the OZ with the CZ, it is convenient to use similar metrics. Therefore, new metrics for the OZ are hereby introduced which characterize the width and the mid point of the OZ. The width of the OZ is defined by the optimal zone width (OZW) while the mid point is defined by the point of mean optimal (PMO) zone. The OZW and PMO are given by Equations (3) and (4), respectively, where up_{OZ} is the upper optimal amplitude and lo_{OZ} is the lower optimal amplitude:

$$OZW = up_{OZ} - lo_{OZ} \tag{3}$$

$$PMO = lo_{OZ} + \frac{OZW}{2} \tag{4}$$

Summarizing, for both zones we defined metrics to characterize the mid point of the zone, the PMC and PMO, for the CZ and the OZ respectively. In the following, the PMC and the PMO will be referred to as "point of mean zone" (PMZ) measures. Similarly, the CZW and the

OZW will be referred to as "zone width" (ZW) measures. Although the PMC may be different from the PMO, we consider the concept behind these measures to be the same, thus allowing us to define both measures as PMZs. The same applies to the concept behind the CZW and the OZW.

3 Method

3.1 Apparatus

The experiment was conducted in the Visual Motion Simulator (VMS) and the Cockpit Motion Facility (CMF), located at NASA Langley Research Center (LaRC) in Hampton, Virginia, USA. The CMF consists of one motion base and three interchangeable simulator cockpits. For this experiment, two different cockpits were used on the CMF, the Generic Flight Deck (GFD) and the Integration Flight Deck (IFD). Figure 1 shows the VMS and CMF motion bases.
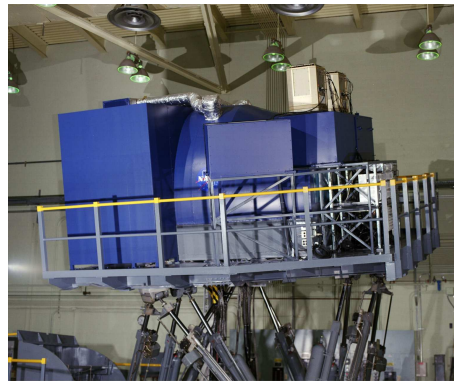
(a) VMS.

(b) CMF.

Figure 1: The VMS and CMF motion bases. (Courtesy of NASA.)

3.1.1 VMS

The VMS has a six degree-of-freedom (DOF), hexapod type, motion base with an actuator stroke of 1.5 m. The maximum displacement, velocity and acceleration in the lateral axis are ± 1.2 m, ± 0.6 m/s and ± 5.9 m/s^2, respectively. For motion control, commands were sent to the motion base at 50 Hz.

The visual system consists of four Wide Angle Collimated (WAC) windows of 1024 by 944 pixels with an update rate of 60 Hz. The front windows provide a field-of-view (FoV) of 65.93 deg horizontal by 45.23 deg vertical. The lateral window on the left-hand side has a FoV of 48.50 deg horizontal by 35.50 deg vertical.

The lateral acceleration of the motion base was measured using Sundstrand QA-900 accelerometers (serial number 1271). These have been tested and calibrated to ± 2g at up to 100 Hz, and have deviations of less than 1000 μg.

3.1.2 GFD

The motion base of the CMF is also a 6 DOF, hexapod motion base, although it is larger and newer than the VMS. The actuator stroke is 1.9 m and the lateral motion limits are ± 1.4 m, ± 1.0 m/s, and ± 6.9 m/s^2 in position, velocity and acceleration, respectively. The motion base was controlled at 50 Hz.

The GFD visual system consists of four WAC windows with an update rate of 60 Hz. The front windows have a horizontal FoV of 46 deg and a vertical FoV of 34 deg. The lateral windows have a FoV of 49 deg horizontal by 37.5 deg vertical. Although the FoV is smaller in this cockpit than in the VMS, the resolution of the screens is higher, with each window having 1280 by 1024 pixels.

The lateral acceleration was recorded with a Honeywell Q-Flex(R) accelerometer (Model QA-700) which was placed under the dynamic platform at the centroid position.

3.1.3 IFD

The IFD cockpit is also part of the CMF, so the motion base description given for the GFD also applies to this simulator.

The visual system is quite different from the GFD and VMS. It consists of a collimated panoramic display, with a horizontal FoV of 200 deg and a vertical FoV of 40 deg. Five projectors are used, each with 1440 by 1024 pixels, and an update rate of 60 Hz.

The interiors of the three simulators are shown in Figure 2.

(a) VMS.   (b) GFD.

(c) IFD.
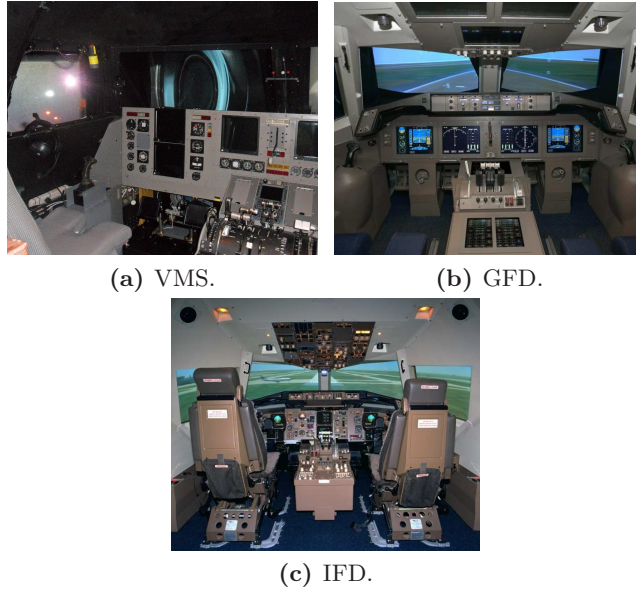
Figure 2: View of the interiors of the three cockpits. (Courtesy of NASA.)

3.2 Experimental design

The experiment had a four way repeated measures design. The independent factors considered were the three simulators described above, the two types of instructions given to subjects (either optimal or coherence zone tuning), two visual stimulus amplitudes, and two stimulus frequencies.

The visual stimulus amplitudes used were 0.5 and 1 m/s^2. These amplitudes were chosen such that the results could be directly compared to previous studies on optimal gain tuning performed in other simulators.

The choice of frequencies was less straightforward. Initially three frequencies of 2, 3, and 5 rad/s were chosen for the GFD and IFD part of the experiment. The lowest frequency of 2 rad/s was the lowest possible frequency to be tested while still remaining within the motion base limits. For the VMS the minimum frequency was 3 rad/s, however, so only two frequencies would be tested in this simulator.

During preliminary tests it became clear that because both coherence zones and optimal gain measurements were being performed, the experimental sessions were too long and there was the risk that subjects would become too tired. For this reason, one of the frequencies was eliminated from the tests in the GFD and IFD. To maintain symmetry with respect to the tests in the VMS, it would have been better to eliminate the 2 rad/s condition. However, it was thought that maintaining this low frequency would allow a more direct comparison to results from other studies that used the same stimulus frequency. Moreover, the larger the

differences between tested frequencies the easier it would be to observe the effect of frequency on the coherence zones. It was then decided to maintain the 2 and 5 rad/s conditions for the GFD and IFD and test the 3 and 5 rad/s conditions in the VMS. With this design, comparison among the three simulators can be done only at the frequency of 5 rad/s.

In each simulator and for each of the conditions, two measurements were taken: during the optimal tuning, one measurement for each of two initial amplitudes of the inertial motion cue; and during the coherence zone measurements, one for the upper thresholds and one for the lower threshold. For each of these measurements three repetitions were made, resulting in a total of 48 experimental trials in each simulator.

3.3   Motion and visual signals

The visual and inertial motion stimuli consisted of sinusoidal signals with amplitude and frequency defined by the experimental conditions described above. The signals were designed such that experimental runs of different frequencies would have the same duration. The length of the motion signals were 2, 4 and 8 periods for the conditions with frequencies of 2 rad/s, 3 rad/s and 5 rad/s, respectively.

These sinusoidal signals were faded in and out to guarantee that the acceleration, velocity and position signals always started and ended at zero. The fade in and fade out parts of the signal are described by Equation (5), where A is the amplitude in m/s^2, ω is the signal frequency in rad/s, and ω_s and ω_c are the smoothing and compensation frequencies, respectively, also in rad/s. Both the smoothing and the compensation frequencies equaled half of the signal frequency.

$$f(t) = \frac{1}{2}A\sin(\omega t) - \frac{1}{2}A\sin(\omega t)\cos(\omega_s t) + A_c \sin(\omega_c t) \qquad (5)$$

The complete motion signal is given by Equation (6) where T is the period of the signal and N is the number of periods in one run. The number of periods does not include the two periods that are necessary to perform the fade in and fade out. Including the fade in and the fade out, the total length of one run was 12.57 seconds.

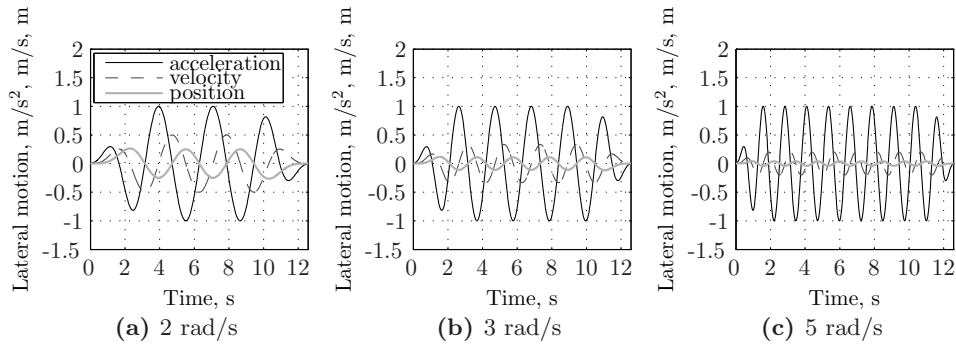$$a(t) = \begin{cases} f(t), & 0 < t \leq T \\ A\sin(\omega t), & T < t \leq (N+1)T \\ f(t-T), & (N+1)T < t \leq (N+2)T \end{cases} \qquad (6)$$

Figure 3 shows examples of complete runs for all three frequencies and an amplitude of 1 m/s^2.

3.4   Procedure

The experiment was divided in three parts. The first part was conducted in the GFD, the second part in the VMS and the third part in the IFD.

Figure 3: Example of the motion signals during one run for the three different frequencies and an amplitude of 1 m/s^2.

Due to simulator scheduling it was not possible to have all simulators available at the same time, so randomization between simulators was not possible. There was one month separating the tests in the GFD and in the VMS and four months between the VMS and the IFD parts. The same subjects were used in all three simulators. The order of the 48 experimental trials performed in each simulator was randomized for every subject. For each subject, the trial order was the same on all three simulators.

In both simulators, the optimal zone experimental block was performed before the coherence zone experimental block for all subjects. This was done to ensure that knowledge regarding a "coherence zone", which is a necessary part of the coherence zone instructions, did not negatively influence subjects' strategy during the optimal zone measurements. After being told that a range of amplitudes exist where motion and visual cues are perceived as coherent although they are not a physical match, subjects could reject the concept of an optimal zone, and the idea that it could be found by further tuning the inertial amplitude of a simulator. This could hinder their motivation to find the "best match" during the optimal zone measurements. Obviously, for the experimental trial in the second and third simulators, subjects were already familiar with both concepts. However, in this case, they have already experienced that indeed both tasks, optimal and coherence zone measurements, are possible to accomplish using the same tuning method.

Subjects were seated in the left-hand seat of the simulator cockpit. The subject wore a headset with active noise cancellation which allowed communication with the experiment supervisor. Three buttons located in the sidestick, which was located on the left side of the participants, were used to record their answers throughout the experimental runs.

For each experimental trial, the visual motion amplitude was kept constant and the inertial motion amplitude was varied throughout a set of runs. For each trial of the optimal zone measurements, the ampli-

13

tude of the first run was randomly selected at an amplitude between 1.4 and 1.6 times the visual amplitude for runs that approach the optimal zone from above or a random value between 0.4 and 0.6 times the visual amplitude for approaching the optimal zone from below. For the coherence zone measurements, the initial inertial amplitude was a random value between 1.1 and 0.9 times the visual amplitude. Before each coherence zone trial started, subjects were informed whether that trial corresponded to a lower or an upper threshold measurement.

At the end of each run within a trial subjects could change the motion of the next run. They did this by pushing a switch button multiple times up or down until they reached a certain number of increments or decrements. The chosen number was shown on a head-down display placed directly in front of the subjects. A positive number meant the next run would have a higher amplitude motion, and a negative number meant a lower amplitude motion. After giving their answer, subjects pressed a second button to signal that they were ready for the next run.

The trial ended when subjects' answers had two consecutive reversals of one increment or decrement, i.e., a sequence of 1, -1, 1, or -1, 1, -1. This indicated that subjects converged to a certain amplitude of motion that could not be increased or decreased anymore. To avoid fatigue, trials were also stopped if subjects reached 30 runs. The size of the increment or decrement was 0.025 times the visual amplitude, which corresponded to 0.0125 m/s^2 for the lowest amplitude condition and 0.050 m/s^2 for the highest amplitude condition.

Before starting the experiment, subjects performed three randomly chosen experimental trials for training purposes.

3.5   Subjects and subjects' instructions

Eight subjects were selected from the employees of the LaRC Flight Simulation Facility. There were seven male participants and one female participant. The subjects' average age was 49 years, ranging between 31 and 64 years old. All eight subjects were able to complete the experiment, and there were no complaints of motion sickness.

The participants were instructed to sit upright and refrain from making head movements throughout the experiment. They were, however, allowed to gaze over the visual scene at will.

Participants were told they were to perform a series of experimental trials which consisted of several runs. In each trial the visual scene would move the same way but the amplitude of the simulator inertial motion would vary between runs depending on their input.

For the optimal zone measurements, subjects were not informed whether the trial was an upper or a lower optimal amplitude measurement. Participants were instructed to find the inertial motion amplitude that, in their opinion, matched the visual amplitude cue the best.

For the coherence zone measurements, subjects were told at the beginning of the trial whether an upper or a lower threshold measurement was being performed. For an upper threshold measurement, subjects were asked to find the strongest inertial motion amplitude that was still perceived as coherent with the visual cue. For a lower threshold measurement they were asked to find the weakest inertial motion amplitude that was still coherent with the visual cue.

For both optimal and coherence zone measurements subjects were instructed to decrease and increase the inertial motion amplitude as many times as needed until they were satisfied with their choice. Subjects were advised to start with increments of 10 or more and decrease the number of increments or decrements at every direction reversal. They were informed of the stopping criteria of the trials.
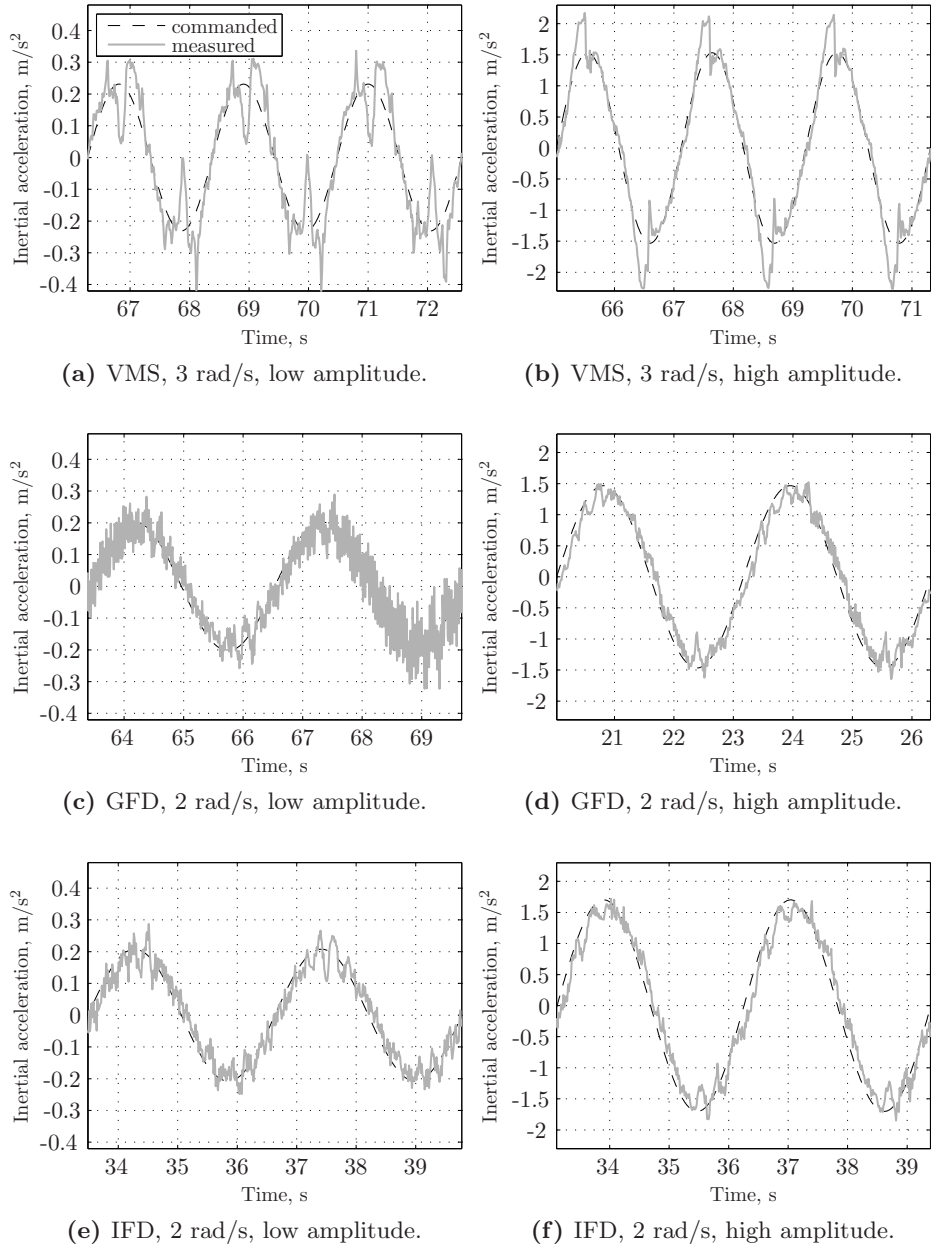
3.6   Motion base performance

To observe the differences in motion base performance between the three simulators, the commanded lateral acceleration was compared to the measured signals for each of the three simulators. Figure 4 and Figure 5 show time histories of the commanded and measured signals for all frequencies at high and low amplitudes. The amplitudes chosen to be plotted are around $0.2\,\mathrm{m/s^2}$ and $1.5\,\mathrm{m/s^2}$ for the commanded signal, and are representative of the limits of the search interval for most subjects.

As can be seen, there were quite some differences in performance between the VMS and the CMF motion bases. The VMS showed a more pronounced "turn around bump" at the low amplitude and low frequency conditions and a clear overshoot at the high amplitude conditions. The low amplitude conditions at a frequency of 5 rad/s seemed to be equally demanding for both motion bases. In these conditions the time histories clearly showed an additional oscillation around 15 rad/s for the VMS and 20 rad/s for the CMF. Although these oscillations were more pronounced at the low amplitude and high frequency conditions, a spectral analysis of the time histories showed that they were present in all other conditions as well.

The data from the CMF motion base also showed oscillations around 180 rad/s, which were stronger with the GFD than with the IFD cabin. The oscillations can clearly be seen in the time histories in Figure 4c and Figure 5c. Although both cockpits were mounted on the same motion base, differences in the mass of the cockpits, if not fully taken into account by the motion base controller, may have affected the overall performance.

Since there were considerable differences between the commanded and the measured motion, the thresholds should be based not on the amplitudes of the commanded signals, but on the amplitudes of the measured signals. However, some care should be taken, since some of the peak amplitudes of the measured signal might have been caused by

(a) VMS, 3 rad/s, low amplitude.

(b) VMS, 3 rad/s, high amplitude.

(c) GFD, 2 rad/s, low amplitude.

(d) GFD, 2 rad/s, high amplitude.

(e) IFD, 2 rad/s, low amplitude.

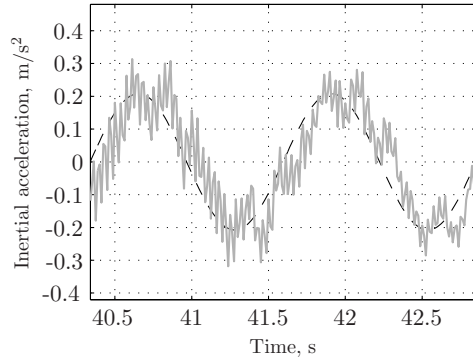**(f)** IFD, 2 rad/s, high amplitude.

Figure 4: Time histories of the commanded and the measured lateral acceleration for frequencies of 3 and 2 rad/s.

16
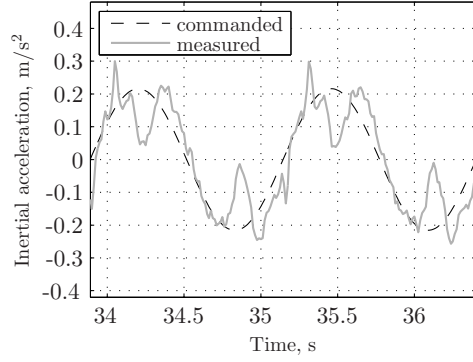
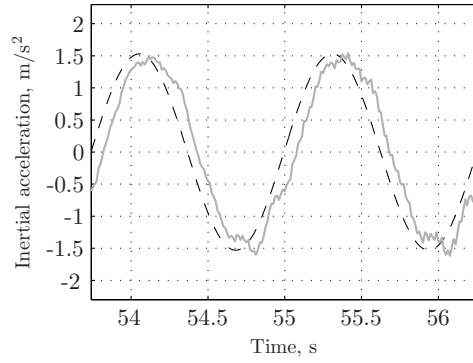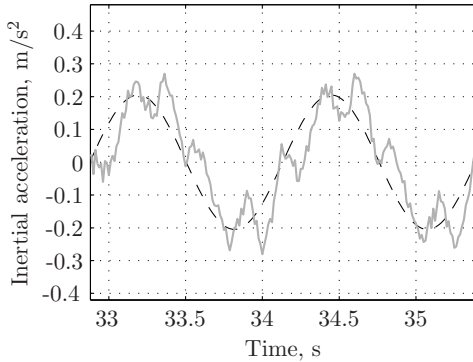**(a)** VMS, 5 rad/s, low amplitude.
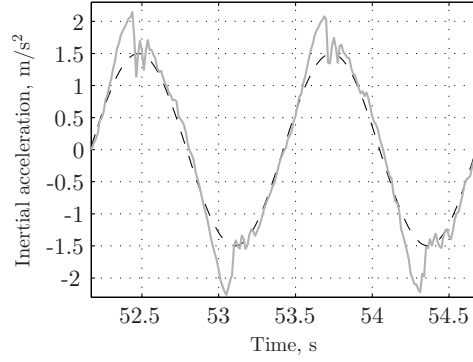
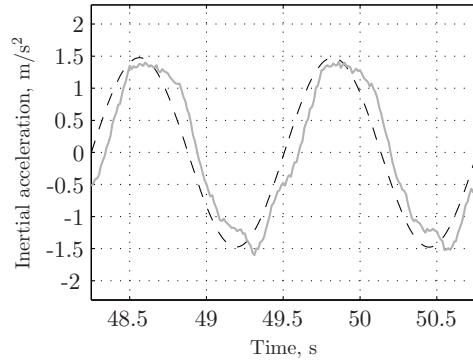**(b)** VMS, 5 rad/s, high amplitude.

(c) GFD, 5 rad/s, low amplitude.

(d) GFD, 5 rad/s, high amplitude.

(e) IFD, 5 rad/s, low amplitude.

(f) IFD, 5 rad/s, high amplitude.

Figure 5: Time histories of the commanded and the measured lateral acceleration for the 5 rad/s frequency.

17

noise inherent to the accelerometer and not motion of the platform.

To preserve the measured accelerations and eliminate high frequency noise that is unlikely to have resulted from the inertial motion of the platform, the measured signals were filtered with a second order filter with a cutoff frequency of 50 rad/s. Examples of the measured signals before and after the filtering are shown in Figure 6. Only examples of the low amplitude runs are plotted, since the differences between the measured and filtered signals are more noticeable in these.

For the coherence zones, the threshold values were determined by averaging the peak amplitude of the last two runs in each trial. For the optimal zone, thresholds were determined by the peak amplitude of the last run. The so determined thresholds were then averaged across the three repetitions of each condition. Especially for the VMS, the differences in peak amplitudes between the commanded and the filtered signals were quite large, so a large difference can be expected between the thresholds if they are determined from the commanded signals or from the filtered signals.

Regarding the IFD and the GFD, the differences in weight of the two cockpits, with the IFD weighting 10% more than the GFD, was expected to slightly influence the motion base performance. However, apart from a high frequency oscillation that is stronger in the GFD than in the IFD, the lateral motion performance of the motion platform was very similar. It is not clear what caused the high frequency oscillation. One hypothesis would be that it is not actually an oscillation of the motion base, but of the measurement unit. The frequency of this oscillation was around 180 rad/s or 28 Hz, which may be too low for electrical noise, but it could be explained by some type of mechanical vibration at the attachment point between the measurement unit and the platform.

3.7   Data analysis

From the coherence zone measurements we obtained inertial amplitudes for the upper (th_{up}) and lower (th_{lo}) thresholds. From these thresholds we obtained the coherence zone width (CZW) and the point of mean coherence (PMC), as defined by Equations (1) and (2), respectively. For the data analysis of the coherence zone measurements, the dependent measures were the PMC and the CZW; the independent variables were the visual amplitude and frequency.

From the optimal zone measurements we obtained inertial amplitudes for the upper (up_{OZ}) and lower (lo_{OZ}) optimal amplitudes. With these, we calculated the point of mean optimal (PMO) zone and the optimal zone width (OZW) as defined by Equations (3) and (4), respectively. For the data analysis of the optimal zone, the dependent measures were the PMO and the OZW; the independent variables were the visual amplitude and frequency.
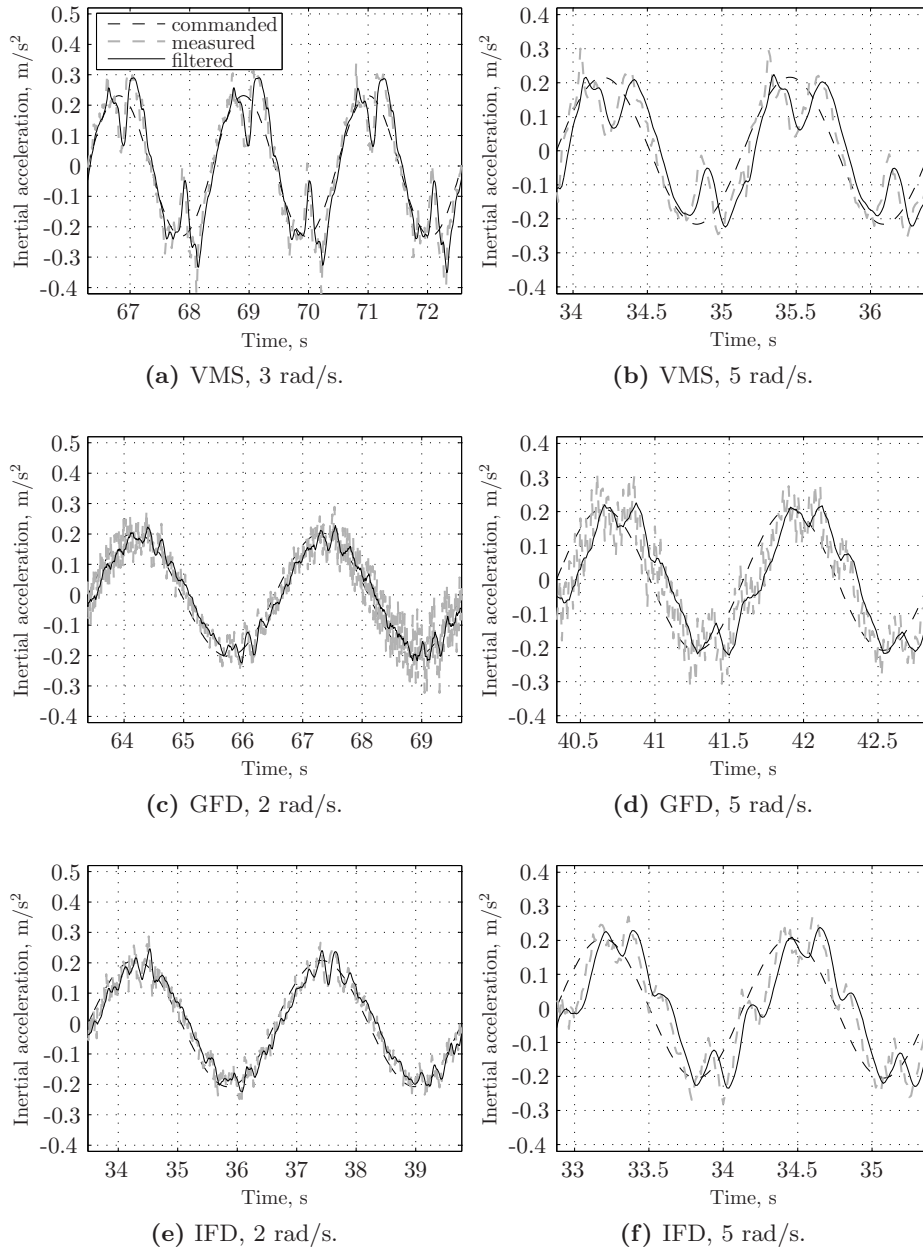
Figure 6: Time histories of the measured and the filtered lateral acceleration signals for all frequencies and low amplitude inertial motion.

19

To compare the OZ with the CZ we calculated their respective 'point of mean zone' (PMZ) and 'zone width' (ZW) metrics. The PMZ for the OZ is given by the PMO while for the CZ it is given by the PMC. Similarly, the ZW for the OZ is given by the OZW while for the CZ it is given by the CZW. The PMZs and the ZWs were then used as the 'dependent measures' when comparing the coherence zone with the optimal zone. The independent variables were then the visual amplitude, the frequency, and the instructions that the subjects got. That is, the difference between the OZ and CZ measurements is examined as a function of the different instructions that the subjects received before conducting the experiment. With the CZ instructions, subjects are expected to converge to inertial amplitudes that are higher or lower than the corresponding visual amplitude. Conversely, for the OZ instructions, subjects are expected to converge to inertial values closer to the visual amplitude. Therefore, it is expected that the inertial amplitudes obtained with the OZ instructions lie within the inertial amplitudes obtained with the CZ instructions.

When comparing both simulators we again used the PMZs and ZWs as dependent measures and the simulator, instructions and visual amplitude as independent variables.

For the statistical analysis we conducted repeated measures analysis of variance (ANOVAs). We considered as highly significant the main effects with a p value lower or equal to 0.01, and as significant the main effects with a p value between 0.01 and 0.05. The statistical analysis were performed with SPSS PASWS 19.

4 Results

4.1 Coherence zones

For the tests in the VMS, the thresholds determined from the commanded signals are shown together with the thresholds determined from the filtered signals in Figure 7.

As can be seen, there was indeed a considerable difference between the commanded signal thresholds and the filtered signals thresholds, especially for the upper thresholds of the high amplitude conditions. Although the difference between commanded and filtered thresholds for the other simulators was negligible, for the sake of consistency, all thresholds were determined from the filtered signals. Therefore, except where explicitly mentioned otherwise, all threshold values presented here were determined from the filtered signals.

Figure 8 shows the determined thresholds for all conditions in the VMS. In this and all following figures, the error bars indicate the 95% confidence interval of the mean.
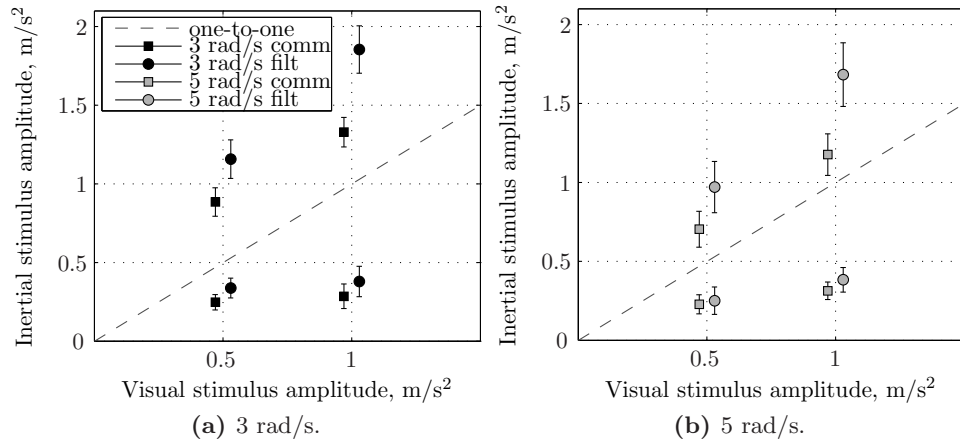
(a) 3 rad/s.

(b) 5 rad/s.

Figure 7: **Upper and lower thresholds based on commanded (comm) and filtered (filt) signals in the VMS. Error bars indicate the 95% confidence interval of the mean.**
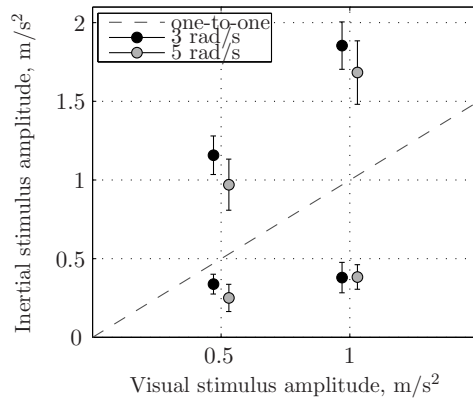

Figure 8: Upper and lower thresholds for the VMS.

For both frequencies and amplitudes of the visual stimulus, the upper and lower thresholds defined a coherence zone that included the one-to-one line. The variation of the lower threshold values across conditions was small, whereas the upper thresholds clearly increased with the visual stimulus amplitude and decreased with frequency.

A repeated measures Analysis of Variance (ANOVA) was performed to investigate whether the observed differences were significant. The results of the analysis are shown in Table 1. All data were normally distributed. Both the frequency and the amplitude had a significant effect on the upper thresholds, but not on the lower thresholds. There were no significant interaction effects.

Table 1: Results of the ANOVA for the measured thresholds in the VMS, where ** is highly significant ($p \leq 0.01$), * is marginally significant ($p \leq 0.05$), and - is not significant ($p > 0.05$).

Independent variables	Dependent measures					
	Lower threshold			Upper threshold		
	df	F	sig.	df	F	sig.
Amplitude	1,7	2.47	-	1,7	48.36	**
Frequency	1,7	1.60	-	1,7	5.59	*
Amplitude × Frequency	1,7	3.07	-	1,7	0.02	-

The effect of frequency, with higher frequencies leading to lower upper thresholds, is similar to what was found for yaw motion in Valente Pais *et al.* [33, 34, 36] and it is in agreement with previous studies that showed that subjects judge motion strength not only on the basis of acceleration but also of jerk [42].

In Valente Pais *et al.* [33] it was argued that the influence of frequency on the yaw coherence zone might be related to the dynamics of the semicircular canals (SCC). The gains applied to the inertial stimulus by the SCC might not be taken into account during the internal comparison of visual and inertial stimuli resulting in a deviation of the Point of Mean Coherence (PMC) from the one-to-one line. If the same rationalization were to be applied to the lateral motion, one would expect a similar but weaker effect, since the gain of the otoliths also increases with frequency [10], but only slightly, for a frequency range between 1 and 10 rad/s. This may help explain the variation in the upper threshold values with increasing frequency, but it is not in agreement with what was found for the lower threshold values.

Surprisingly, the lower thresholds were not affected by the stimulus frequency. One explanation for this fact might be the performance of

the motion platform at the low amplitudes. The crosstalk might have masked the lateral motion to such an extent that it hindered subjects in their task. One other explanation could be the relatively lower resolution of the measurement method at the lower amplitudes. In the experimental setup, the minimum amplitude intervals that are tested depend on the amplitude of the visual stimulus, so they are the same for the lower and the upper threshold trials. A small enough amplitude interval at the higher amplitude runs may be too large to capture the slight differences in lower threshold measurements. Of course, it may happen that for these specific combinations of lateral motion amplitudes and frequencies the lower thresholds of the perceived coherence zone are indeed very similar.

The amplitude of the visual stimulus also had a significant effect on the upper thresholds but not on the lower thresholds. Again, the lower threshold runs might have been affected by the resolution of the experimental method. Although not immediately observable from the upper and lower threshold plots, very similar to what happens for yaw coherence zones, the coherence zone bends down with respect to the one-to-one line. This effect is easier to see by looking at the PMC values. For the higher amplitude the PMC value is still higher than 1 m/s^2, but it is much closer to the one-to-one line than for the lower amplitude.

The thresholds determined in the GFD and IFD are shown in Figure 9. Similarly to the results from the VMS, the visual stimulus amplitude and frequency had a more noticeable effect on the upper thresholds than on the lower thresholds. For both simulators, there was a very small increase in the lower thresholds for the higher amplitude and a slight decrease for the higher frequency conditions. The same trend can be seen for the upper thresholds, but here the differences are much larger. The upper thresholds measured in the GFD were slightly lower than the ones measured in the IFD, and the lower thresholds were slightly higher.

To investigate whether these effects were significant, an ANOVA was performed on the data. Table 2 shows the results of this analysis. Only the main effects and significant interactions are shown. The effect of amplitude and frequency on the lower threshold values was not significant. Moreover, the lower thresholds from the two simulators were not significantly different. The upper threshold values were significantly affected by the simulator, amplitude and frequency factors. In addition, the effect of frequency on the upper thresholds was larger on the IFD than on the GFD, as is confirmed by the significant interaction effect found between simulator and frequency.

The influence of frequency and amplitude on the thresholds followed the same trends as the ones seen in the VMS. The higher frequency conditions resulted in lower values, although that effect was only statistically significant for the upper thresholds. The fact that also in these two

(a) GFD.

(b) IFD.
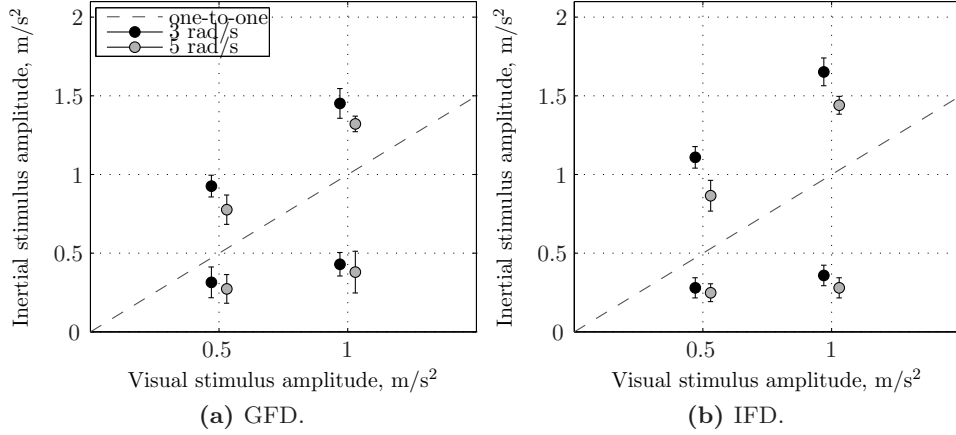
Figure 9: Upper and lower thresholds for the GFD and the IFD.

Table 2: Results of the ANOVA for the measured thresholds in the GFD and IFD, where ** is highly significant (p$\leq$ 0.01), * is marginally significant (p$\leq$ 0.05), and - is not significant (p$>$ 0.05).

Independent variables	Dependent measures					
	Lower threshold			Upper threshold		
	df	F	sig.	df	F	sig.
Simulator	1,7	2.48	-	1,7	24.84	**
Amplitude	1,7	2.56	-	1,7	156.07	**
Frequency	1,7	2.96	-	1,7	21.77	**
Simulator $\times$ Frequency	1,7	0.05	-	1,7	7.37	*

24

simulators the different conditions did not significantly affect the lower thresholds indicates that either the amplitudes and frequencies chosen were not different enough, or indeed that the measuring method lacks resolution at the lower amplitudes. Since this is a result that is constant across simulators, the probability that it is related to a specific simulator configuration, is small.

The measured thresholds from all three simulators can be compared only for the highest frequency, since in the VMS the lower frequency was 3 rad/s and not 2 rad/s as in the GFD and IFD. The upper and lower thresholds at 5 rad/s and at the two amplitudes for all simulators are shown in Figure 10. For comparison purposes both the thresholds calculated from the commanded and from the measured signals are shown.

(a) Commanded signals.   (b) Measured signals.
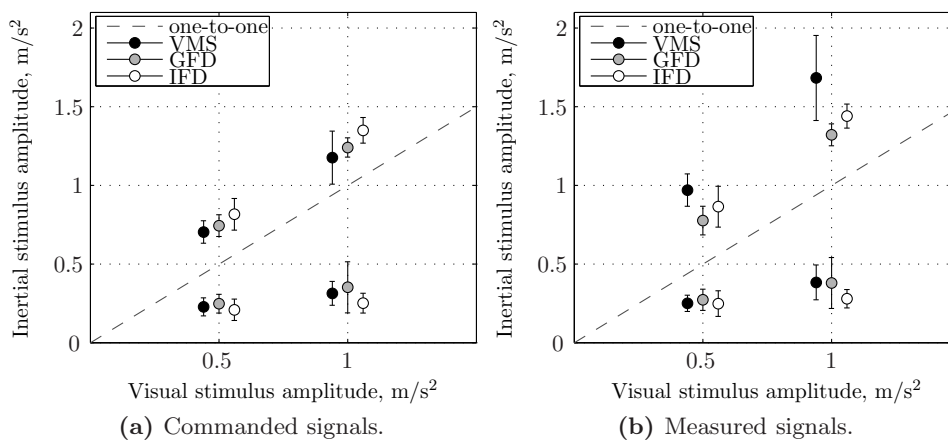
Figure 10: Upper and lower thresholds, for the 5 rad/s frequency conditions, in the VMS, GFD and IFD, obtained from commanded and measured signals.

The lower thresholds did not vary much from one simulator to the other. The largest differences were seen in the upper threshold values. The VMS showed the highest values, especially for the conditions with the $1\,\mathrm{m/s^2}$ amplitude. The GFD showed the lowest upper thresholds. An ANOVA was performed on the data. The results are shown in Table 3. The lower thresholds were not significantly different across conditions and simulators. The simulator and the amplitude had a significant effect on the upper thresholds. Although the larger difference seemed to be between the VMS and the other two simulators, a post-hoc pairwise comparison, using Bonferroni adjustments for multiple comparisons, showed that the VMS and the IFD were not significantly different, but the GFD was significantly different from the VMS and the IFD.

The coherence zones limited by the upper and lower thresholds can also be represented in terms of a PMC and a Coherence Zone Width

Table 3: Results of the repeated measures ANOVA for the measured thresholds in all three simulators for a stimulus frequency of 5 rad/s, where ** is highly significant ($p \leq 0.01$), * is marginally significant ($p \leq 0.05$), and - is not significant ($p > 0.05$).

Independent variables	Dependent measures					
	Lower threshold			Upper threshold		
	df	F	sig.	df	F	sig.
Simulator	2,14	1.32	-	1.19,10.18[a]	7.96	*
Amplitude	1,7	3.15	-	1,7	72.64	**
Simulator × Amplitude	2,14	1.03	-	12,14	2.03	-

[a] Greenhouse-Geisser sphericity correction applied.

(CZW). Figure 11 shows the results in the three simulators in terms of PMC and CZW.

(a) Point of mean coherence. (b) Coherence zone width.
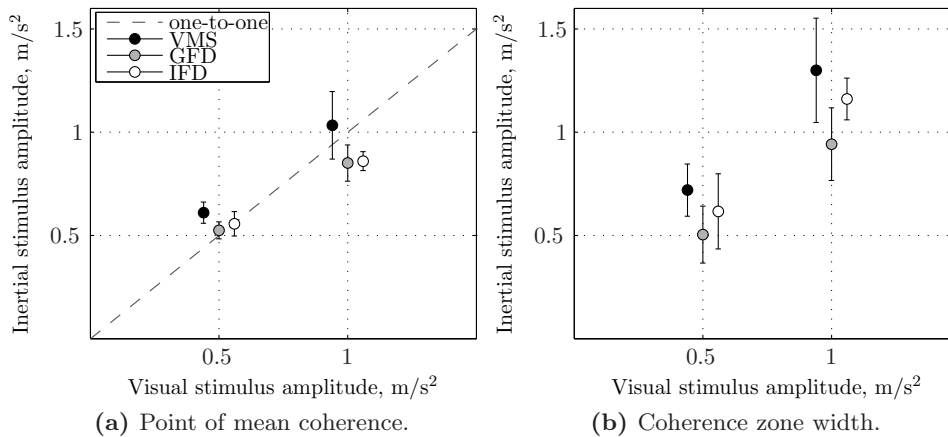
Figure 11: Measured coherence zones.

The PMCs increased with amplitude, approximately following the one-to-one line, although for the higher amplitude they were slightly lower with respect to this line than for the lower amplitude conditions. The VMS had the highest PMCs, which is to be expected, given that the upper thresholds were also much higher in this simulator. The CZWs were also larger for the higher amplitude conditions. The VMS had the wider coherence zones, followed by the IFD. The GFD presented the narrowest zones.

The ANOVA results, shown in Table 4, indicate that the effect of

amplitude was significant on both the PMC and the CZW. The simulator factor was also significant on both metrics, although it was not possible to statistically differentiate the CZWs in the three simulators using a post-hoc pairwise comparison (again using Bonferroni adjustment). For the PMC the post-hoc tests showed a significant difference between the VMS and the GFD, but not between the VMS and the IFD and between the GFD and the IFD.

Table 4: **Results of the repeated measures ANOVA for the PMC and CZW in all three simulators for a stimulus frequency of 5 rad/s, where ** is highly significant ($p \le 0.01$), * is marginally significant ($p \le 0.05$), and − is not significant ($p > 0.05$).**

Independent variables	Dependent measures					
	PMC			CZW		
	df	F	sig.	df	F	sig.
Simulator	$1.20, 8.41^{a}$	5.39	*	2,14	7.44	**
Amplitude	1,7	108.49	**	1,7	24.82	**
Simulator $\times$ Amplitude	$1.95, 8.37^{a}$	1.67	−	2,14	1.51	−

[a] Greenhouse-Geisser sphericity correction applied.

4.2 Optimal zone

Figure 12 shows the average upper and lower optimal amplitudes obtained for the VMS simulator based on the commanded and filtered signals. Similar to what was observed for the coherence zone measurements, the filtered amplitudes were higher than the commanded amplitudes. This amplitude difference is more noticeable for the upper optimal amplitude because the VMS turnaround peaks increase with the increase of the commanded amplitude. To be consistent with the coherence zone analysis, the optimal zone results were obtained using the filtered amplitudes.

Figure 13 shows the mean amplitudes defining the optimal zone for the VMS simulator. These mean amplitudes increased with the increase of the visual stimulus amplitude. On the other hand, the mean amplitudes of the optimal zone decreased with the increase of the visual stimulus frequency. This frequency difference is also observed in the optimal zone intersection with the one-to-one line. The 3 rad/s optimal zone contained the one-to-one line at the 0.5 m/s^2 amplitude, with a lower optimal gain close to 0.5 m/s^2, but not at the 1 m/s^2 amplitude, where both the upper and lower optimal amplitudes were below the one-

(a) 3 rad/s.
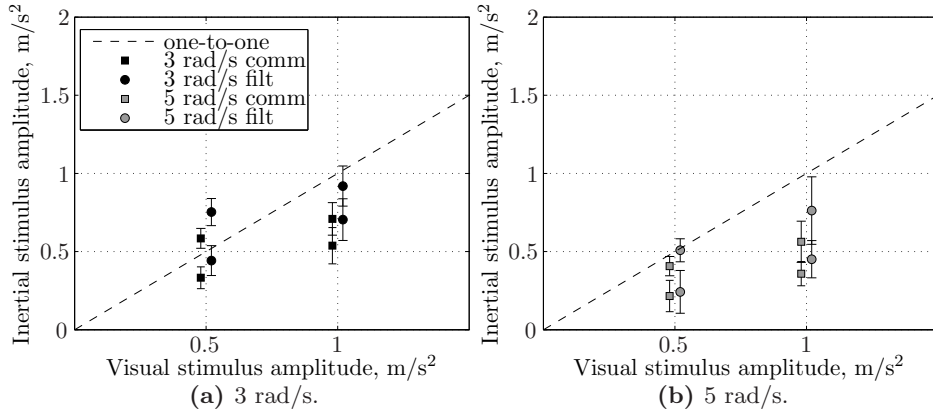
(b) 5 rad/s.

Figure 12: Upper and lower optimal amplitudes based on commanded (comm) and filtered (filt) signals in the VMS. Error bars indicate the 95% confidence interval of the mean.

to-one line. The 5 rad/s optimal zone also contained the one-to-one line at the 0.5 m/s^2 amplitude but the upper optimal gain was close to 0.5 m/s^2. The upper and lower optimal amplitudes were again lower than the one-to-one line at the 1 m/s^2 amplitude.
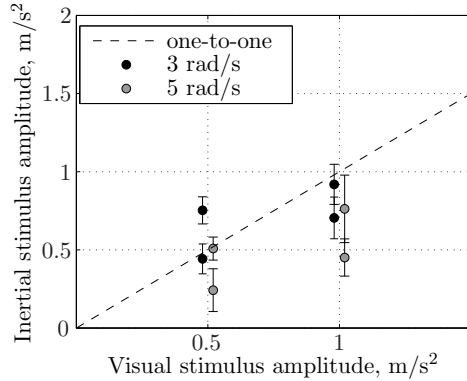
Figure 13: Upper and lower optimal amplitudes for the VMS. Error bars indicate the 95% confidence interval of the mean.

Figure 14 shows the optimal zone obtained for the GFD and IFD simulators. Similarly to the VMS, the mean amplitudes of the optimal zone increased with the increase of the visual stimulus amplitude, both for the GFD and IFD. Again, for both simulators the mean amplitudes of the optimal zone decreased with the increase of the visual stimulus frequency. Additionally, the IFD optimal zone had higher amplitudes than the GFD optimal zone both for the stimulus with 2 and 5 rad/s. The GFD 2 rad/s optimal zone contained the one-to-one line at the 0.5

Table 5: Results of the repeated measures ANOVA for the measured optimal gain amplitudes in the VMS, where ** is highly significant (p≤ 0.01), * is marginally significant (p≤ 0.05), and − is not significant (p> 0.05).

Independent variables	Dependent measures					
	Lower optimal amplitude			Upper optimal amplitude		
	df	F	sig.	df	F	sig.
Amplitude	1,7	14.89	**	1,7	10.07	*
Frequency	1,7	34.50	**	1,7	13.41	**
Amplitude × Frequency	1,7	0.98	−	1,7	1.24	−

m/s^2 amplitude but was lower than it at the 1 m/s^2 amplitude. The 5 rad/s optimal zone of this simulator was always below the one-to-one line. The IFD, on the other hand, had an optimal zone at 2 rad/s that was higher than the one-to-one line at the 0.5 m/s^2 amplitude and contained the one-to-one line at the 1 m/s^2 amplitude. The IFD 5 rad/s optimal zone contained the one-to-one line at the 0.5 m/s^2 amplitude but was lower than it at the 1 m/s^2 amplitude.

(a) GFD. (b) IFD.

Figure 14: Upper and lower optimal amplitudes for the GFD and the IFD. Error bars indicate the 95% confidence interval of the mean.
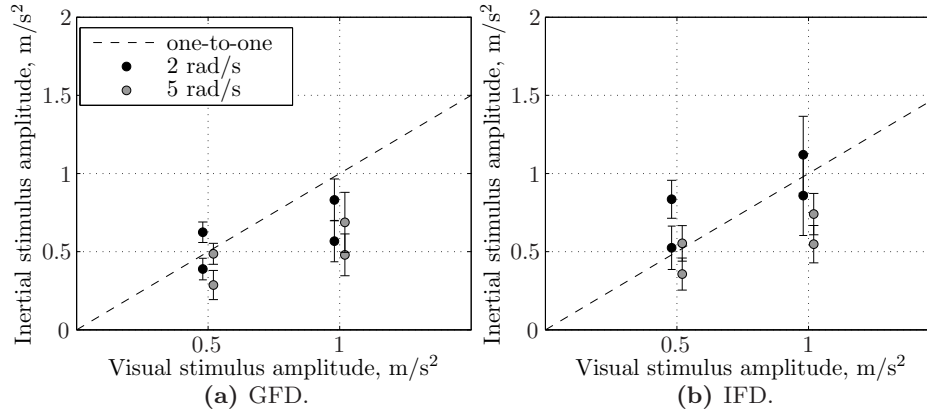
In this section we compared the three different simulators using the optimal zone measurements. This comparison was performed for the stimuli with a frequency of 5 rad/s since these were shared by the three motion-based simulators used in this study. Figure 15 shows that, except for the VMS simulator, the filtered and commanded signals were

Table 6: Results of the repeated measures ANOVA for the measured optimal gain amplitudes in the GFD and IFD, where ** is highly significant (p≤ 0.01), * is marginally significant (p≤ 0.05), and − is not significant (p> 0.05).

Independent variables	Dependent measures					
	Lower optimal amplitude			Upper optimal amplitude		
	df	F	sig.	df	F	sig.
Simulator	1,7	5.32	−	1,7	5.72	*
Amplitude	1,7	19.53	**	1,7	14.78	**
Frequency	1,7	8.23	*	1,7	15.53	**

very similar. As seen before (Figure 12), the VMS simulator commanded signals have smaller amplitudes than the filtered signals. For the commanded signals, we observe that the VMS optimal zone has the lowest amplitudes whereas the IFD optimal zone has the highest amplitudes. For the filtered signals, while the lower optimal amplitudes follow a similar trend to the one observed for the commanded signals, with the VMS having the lowest lower optimal amplitude and the IFD the highest, the amplitude increase observed on the VMS filtered signals generated an upper optimal amplitude for the VMS similar to the one observed for the IFD.

(a) Commanded signals

(b) Measured signals
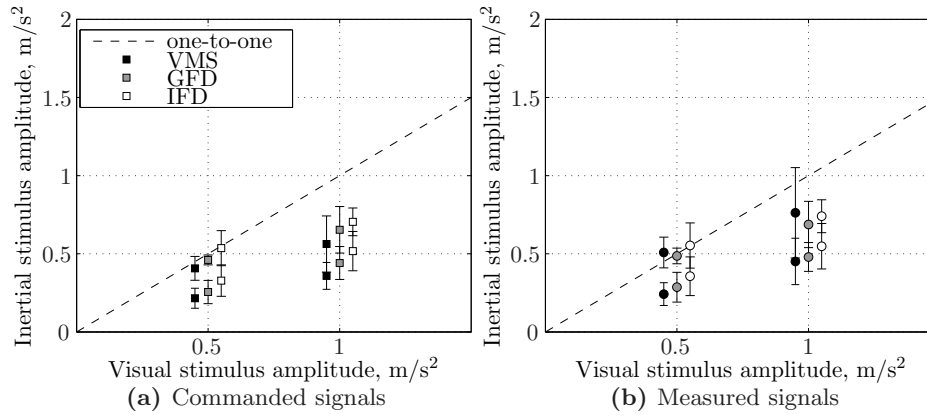
Figure 15: Upper and lower optimal amplitudes based on commanded (comm) and filtered (filt) signals in the VMS, GFD, and IFD. Error bars indicate the 95% confidence interval of the mean.

Figure 16 shows the point of mean optimal zone (PMO) and the

Table 7: Results of the repeated measures ANOVA for the measured optimal amplitudes in all three simulators for a stimuli frequency of 5 rad/s, where ** is highly significant (p≤ 0.01), * is marginally significant (p≤ 0.05), and − is not significant (p> 0.05).

| Independent variables	Dependent measures					
	Lower optimal amplitude			Upper optimal amplitude		
	df	F	sig.	df	F	sig.
Simulator	1.18,8.23[a]	2.10	−	1.09,7.65[a]	0.282	−
Amplitude	1,7	12.91	**	1,7	8.51	*
Simulator × Amplitude	2,14	0.06	−	2,14	0.61	−

[a] Greenhouse-Geisser sphericity correction applied.

optimal zone width (OZW) for the VMS, GFD, and IFD. The filtered signals were used in this figure. Overall, we observe that the PMOs for the 0.5 m/s^2 stimulus were closer to the one-to-one line than the 1 m/s^2 PMOs. The IFD PMO is higher than the VMS and GFD PMOs for the 0.5 m/s^2 stimulus. However, for the 1 m/s^2 stimulus the IFD PMO was approximately the same as the VMS PMO but it was still higher than the GFD PMO. The OZW from all simulators was approximately constant when the stimulus amplitude increased from 0.5 to 1 m/s^2. The VMS OZWs where larger than the GFD and IFD OZWs, which were approximately the same. The larger OZW on the VMS is related with the increase of the upper optimal amplitude observed in the filtered data (Figure 15b).

Table 8: Results of the repeated measures ANOVA for the PMO and OZW in all three simulators for a stimuli frequency of 5 rad/s, where ** is highly significant (p≤ 0.01), * is marginally significant (p≤ 0.05), and − is not significant (p> 0.05).

Independent variables	Dependent measures					
	PMO			OZW		
	df	F	sig.	df	F	sig.
Simulator	1.08,7.53[a]	0.61	−	2,14	1.67	−
Amplitude	1,7	12.84	**	1,7	0.07	−
Simulator × Amplitude	2,14	0.41	−	2,14	0.28	−

[a] Greenhouse-Geisser sphericity correction applied.

(a) Point of mean optimal gain **(b)** Optimal zone width
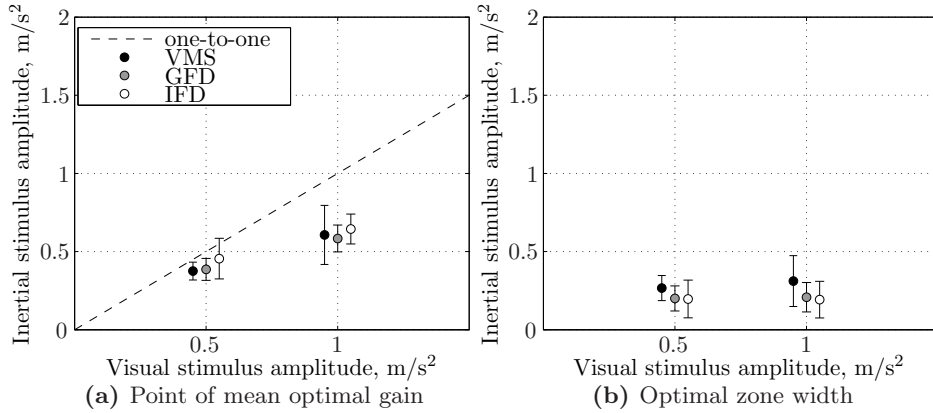
Figure 16: Optimal zone measurements for the VMS, GFD, and IFD. Error bars indicate the 95% confidence interval of the mean.

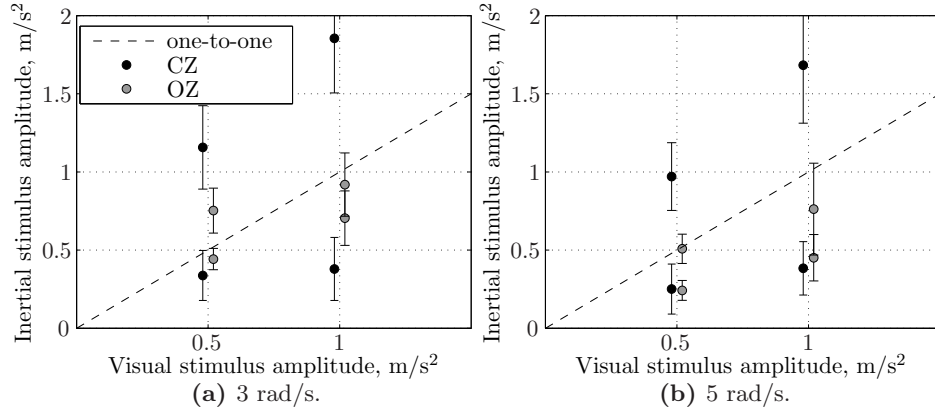## 4.3 Coherence zone versus optimal zone

To compare the two instructions given to the subjects (coherence and optimal zone), we compared the lower threshold with the lower optimal amplitude and the upper threshold with the upper optimal amplitude. Therefore, statistical differences in these boundaries would identify differences between the two instructions. For clarity, the dependent measure "lower boundaries" is used for the comparison between the lower threshold and the lower optimal amplitude whereas the dependent measure "upper boundaries" is used for the comparison between the upper threshold and the upper optimal amplitude.

The comparison between the two instructions was done for the three simulators used in this study. Figures 17, 18, and 19 show the comparison between the coherence and optimal zone for the VMS, GFD, and IFD, respectively. The lower optimal amplitude and the lower thresholds reveal similar lower boundaries for the VMS and GFD simulators.

In fact, in these simulators (see Table 9 and Table 10) we found no statistical differences between the two lower boundaries. For the IFD, however, Figure 19 shows that the lower optimal amplitude is higher than the lower threshold, a significant result as shown in Table 11.

The upper boundaries showed the same trend for the three simulators, where the upper optimal amplitude was higher than the upper threshold. This result, as shown by the respective statistical analysis in Table 9, Table 10, and Table 11, was highly significant for all the simulators in this study.

The consequence of both instructions having similar lower boundaries but different upper boundaries is shown in Figure 20, Figure 21, and Figure 22. Here, we observe that the CZW increases with the visual

Figure 17: Coherence zone and optimal zone in the VMS. Error bars indicate the standard error of the mean.
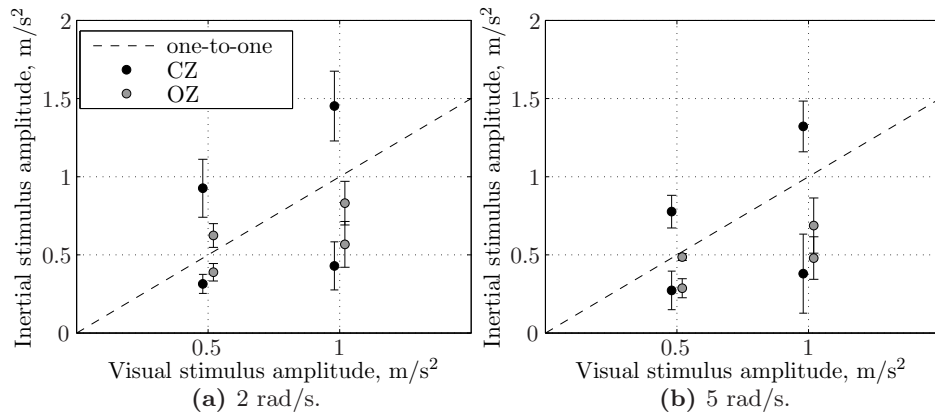
Figure 18: Coherence zone and optimal zone in the GFD. Error bars indicate the standard error of the mean.
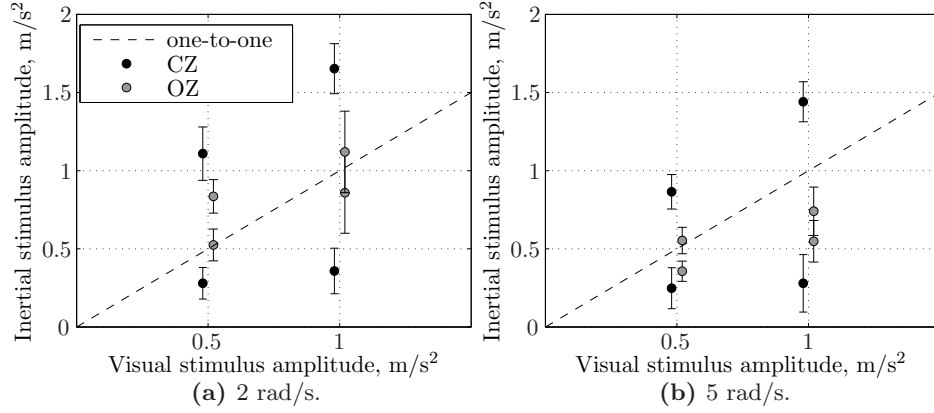
Figure 19: Coherence zone and optimal zone in the IFD. Error bars indicate the standard error of the mean.

Table 9: Results of the repeated measures ANOVA for the measured thresholds and optimal amplitudes in the VMS, where ** is highly significant ($p \leq 0.01$), * is marginally significant ($p \leq 0.05$), and - is not significant ($p > 0.05$).

| Independent variables | Dependent measures | | | | | |
| | Lower boundaries | | | Upper boundaries | | |
	df	F	sig.	df	F	sig.
Instruction	1,7	2.16	–	1,7	14.76	**
Frequency	1,7	17.57	**	1,7	11.30	*
Amplitude	1,7	9.39	*	1,7	46.72	**
Instruction × Frequency	1,7	33.13	**	1,7	0.10	–
Instruction × Amplitude	1,7	8.75	*	1,7	21.50	**

Table 10: Results of the repeated measures ANOVA for the measured thresholds and optimal amplitudes in the GFD, where ** is highly significant (p≤ 0.01), * is marginally significant (p≤ 0.05), and - is not significant (p> 0.05).

| Independent variables | Dependent measures | | | | | |
| | Lower boundaries | | | Upper boundaries | | |
	df	F	sig.	df	F	sig.
Instruction	1,7	1.25	–	1,7	24.03	**
Frequency	1,7	4.41	–	1,7	18.49	**
Amplitude	1,7	7.53	*	1,7	101.36	**
Instruction × Amplitude	1,7	0.89	–	1,7	20.13	**

Table 11: Results of the repeated measures ANOVA for the measured thresholds and optimal amplitudes in the IFD, where ** is highly significant (p≤ 0.01), * is marginally significant (p≤ 0.05), and - is not significant (p> 0.05).

| Independent variables | Dependent measures | | | | | |
| | Lower boundaries | | | Upper boundaries | | |
	df	F	sig.	df	F	sig.
Instruction	1,7	11.01	*	1,7	29.19	**
Frequency	1,7	7.26	*	1,7	21.76	**
Amplitude	1,7	14.60	**	1,7	104.19	**
Instruction × Amplitude	1,7	20.45	**	1,7	16.00	**

stimulus amplitude whereas the OZW remains approximately the same, a result caused by having an upper threshold that is higher and has a steeper slope when increasing with the visual amplitude than the upper optimal gain.
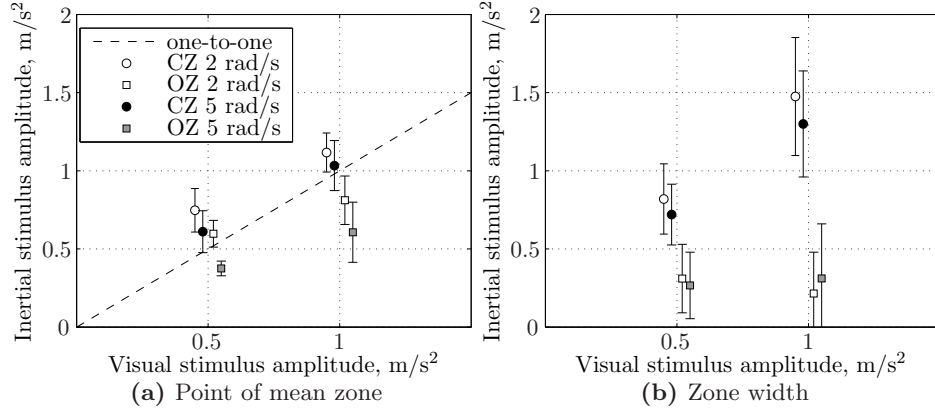
Figure 20: Zone measurements for the VMS. Error bars indicate the standard error of the mean.
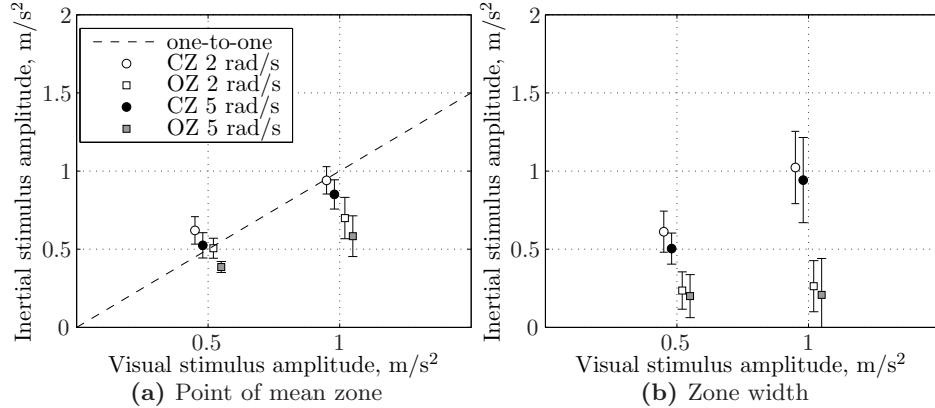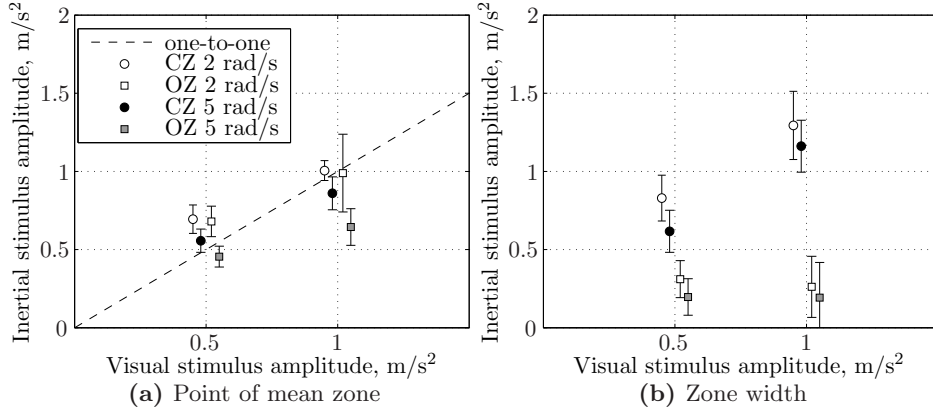

Figure 21: Zone measurements for the GFD. Error bars indicate the standard error of the mean.

5 Discussion

5.1 Coherence zone versus optimal zone

In this experiment we measured perception coherence zones and optimal zones. As was also found in a previous study [35], the optimal zone

(a) Point of mean zone

(b) Zone width

Figure 22: Zone measurements for the IFD. Error bars indicate the standard error of the mean.

measurements did not result in one single value, but in a zone bounded by an upper and a lower limit. For comparison purposes, this optimal zone was defined in terms of point of mean optimal zone (PMO) and optimal zone width (OZW), similar to what was done in other studies [33, 34] for coherence zones, which were defined in terms of point of mean coherence (PMC) and coherence zone width (CZW).

The PMO and PMC both increased with the visual stimulus amplitude and decreased with the visual stimulus frequency. These trends agree well with those reported for optimal zone measurements in sway [35] and coherence zone measurements in yaw [33, 34].

The PMO and PMC both increased with visual stimulus amplitude. For the lowest amplitude the PMCs and PMOs were close to the one-to-one line and for the highest amplitude they were both below this line. This decrease with respect to the one-to-one line was more evident for the PMO.

The PMC was generally closer to the one-to-one line than the PMO. The coherence zone upper threshold was always above the one-to-one line, whereas the upper optimal amplitude crosses the one-to-one line for the 2 rad/s conditions and is below the one-to-one line for the 5 rad/s conditions. Careful observation of the limits for both zones shows that this difference was caused mainly by the upper threshold and upper optimal amplitude since the lower bounds of both zones were similar.

The OZW was significantly lower than the CZW. The CZW was affected by the visual amplitude and frequency, with higher amplitudes leading to wider zones and higher frequencies leading to narrower zones. The OZW was unaffected by these two independent variables. The OZW remained approximately the same (around $0.23\ m/s^2$) for all the experimental conditions. No reason could be found as to why the OZW was

unaffected by frequency and amplitude whereas the CZW was affected by these variables.

As explained above, the lower limits of the CZ and OZ where similar whereas the OZ upper limits were considerably smaller than the CZ upper limits. This resulted in an OZ that covered the lower amplitude values of the CZ. The OZ was thus contained within the CZ, as if there was a subset of coherent inertial and visual cues that was perceived as a "better match".

Together, the coherence and optimal zones defined three regions: within the optimal zone, outside the optimal zone and within the coherence zone, and outside the coherence zone. These three regions can be considered as a gradient of accepted motion ranging from best (within the optimal zone) to worst (outside the coherence zone) motion. These could be compared to the three fidelity regions (low, medium and high) of a Sinacori plot [43], which are commonly used to classify motion cueing algorithms.

It is not clear what perception mechanism allows subjects to distinguish between a coherent and an optimal region. Two different hypotheses can be posed to explain the differences.

First, the different initial inertial amplitudes could have created different paradigms when measuring the two zones. For the coherence zone measurements, subjects started with similar inertial and visual amplitudes and their objective was to increase or decrease the inertial amplitude until a difference between the inertial and visual amplitude was noticed. Conversely, for the optimal zone measurements, subjects started from different inertial and visual amplitudes and their objective was to change the inertial amplitude until the two stimuli were perceived as equal. Although both tasks sound similar, asking for differences between two stimuli appears to create a different result than asking whether two stimuli are equal.

Different results for similar tasks were also found when measuring thresholds for linear motion [5, 10, 44]. Here, subjects were asked to indicate when they perceived motion and when they stopped perceiving motion. In the first case, the motion profile was a sinusoid with amplitude increasing from zero to a supra-threshold value whereas in the second case the motion profile was a sinusoid with its amplitude decreasing from a supra-threshold value to zero. The amplitude at which motion was detected was significantly higher than the value at which subjects stopped perceiving motion.

Second, what could also have led to the differences between the two zones was what may be referred to as "tuning for comfort". Higher inertial amplitudes can be more uncomfortable for the subjects than lower inertial amplitudes. For the optimal zone, subjects were asked to find the best match between visual and inertial information. It could happen that this best match was not where the visual amplitude was equal

to the inertial amplitude but rather the one that felt most comfortable, that is, 'less arousing' inertial amplitude which was *still* perceived as coherent with the visual motion. Such an approach would lead to a PMO lower than the PMC, since for the coherence zone measurements subjects were looking for the boundary of the coherence and not for the most comfortable motion.

This second explanation agrees with the results: PMOs were significantly lower than the PMCs and the optimal zone excluded only the higher inertial amplitudes within the coherence zone.

5.2 Comparing simulators

The three motion simulators used in this experiment combine two types of visual systems, WAC windows and collimated panoramic display, and two different motion bases. Both motion bases are hexapods, but the VMS is a considerably older platform than the motion base of the GFD and IFD (CMF). The performance of the motion bases were monitored by looking at the commanded and measured motion signal.

5.2.1 VMS and CMF: comparing motion base performance

As was to be expected, the older motion platform, the VMS, showed larger turnaround "bumps". The intensity of these bumps increased with the amplitude of the commanded signal. However, in relative terms, the bump was worse at lower amplitudes. This situation was known a priori and the worse performance of the motion base was thought to have an influence especially on OZ and CZ lower limits, since here the amplitudes of the inertial motion were lower. It was thought that the large turnaround bump could increase the overall perception of strength of the inertial motion, leading the subjects to tune down the motion for both high and low amplitudes.

However, at the very low amplitudes, possible crosstalk (motion in other DOFs) might mask the inertial lateral motion, which could lead subjects to tune the motion up, such that motion in the lateral DOF could be distinguished from the crosstalk. The fact that both the coherence zone lower thresholds and the lower optimal amplitudes were not significantly different across simulators shows that if any of these issues played a role, they either canceled each other out, or the effect was too small to be measurable.

The turnaround bump might also have influenced the OZ and CZ upper limits in the VMS. The values obtained from the commanded signals were clearly lower than the ones computed from the measured and filtered signals. The upper thresholds from the commanded signals were in fact lower than the ones obtained in the other two simulators, but when using the measured signals, the peak amplitudes due to the

turnaround bump resulted in higher threshold values. For the upper optimal amplitudes the same trend could be observed, but the difference between the commanded and filtered values was smaller.

On the one hand, one might say that including the peak amplitude of the turnaround bump into the calculation is wrong because it artificially raises the threshold or optimal amplitude value. On the other hand, it is also incorrect to base the values on the peak amplitude of the commanded signals instead of the measured signals when the difference is so large. It was considered that presenting the results in terms of actual measured amplitudes was the most correct.

When comparing the CZ commanded upper threshold values in the VMS to the ones in the GFD, which has the same type of visual system, one might argue that if the turnaround bump was the cause of lower values, then considering the peak amplitude of the turnaround bump in the threshold computation should result in similar thresholds. The fact that the measured thresholds were in fact higher than the ones in the GFD, indicate that although the turnaround bump influenced subjects' perceived motion strength, it did not account for the whole difference between the VMS and the GFD.

The turnaround bump represents a high-frequency component of the motion signal. Subjects perhaps based their CZ judgment on the lower frequency component of the signal and took the turnaround bump only partially into consideration.

The upper optimal amplitudes were not significantly different across simulators indicating that perhaps here the effect of the turnaround bump was negligible. One reason for this might be the fact that during the measurement of the upper limits of the OZ, the amplitude of the inertial motion was generally lower than during the measurements of the CZ. At lower amplitudes, the absolute value of the turnaround bump is also smaller, rendering it perhaps negligible.

5.2.2   GFD and IFD: comparing different visual systems

Unlike the VMS, the difference between the commanded and measured signals peak amplitudes in the IFD and GFD simulators was small, which resulted in very similar commanded and measured threshold values.

Contrary to the lower limits, the upper limits were different between the two simulators for both the CZ and the OZ. The IFD presented higher upper limits than the GFD. When looking at the motion platform performance, the larger differences between simulators were observed at the lower amplitudes. Any differences in the results that would derive from the motion base would then be expected to be more accentuated at the lower limits. However, it is precisely in the upper limits that significant differences are seen. This indicates that the differences found between the limit values were probably due to the visual system.

Chung *et al.* [45] showed that collimation greatly influenced subjects'

perception of lateral velocity and a larger field-of-view improved position control during a hover task. Both the IFD and the GFD have collimated displays, but the IFD has a panoramic display whereas the GFD has four WAC windows. For a subject sitting in the left-hand seat of the simulator only two of those windows provide visual stimulation. This greatly decreases the field-of-view which might lead to an underestimation of the visual cue amplitude in the GFD relative to the IFD. The effect of this underestimation is not observed on the lower limits, which, as mentioned before, might be related to a lack of resolution of the measurement method at low amplitudes.

The CZ thresholds measured in the IFD resulted in a wider coherence zone, although the point of mean coherence was not significantly different between simulators. The larger panoramic display of the IFD favors the onset and strength of vection [46–49] which can lead to a stronger sense of self motion, which in turn allows larger inertial amplitudes before subjects detect some mismatch between the visual and the inertial cue. One can even say that the IFD has a more convincing display, that allows the inertial cue amplitude to divert further from the visual cue before it is noticed by subjects.

However, for the OZ measurements, the IFD did not result in a wider zone. Although the lower optimal amplitudes did not change significantly across simulators, they did change enough to maintain the width of the OZ similar for both simulators. Both lower and upper limits varied with the IFD presenting higher values. This shows that although a more convincing display might allow for a larger mismatch between the visual and the inertial cues, the zone of optimal values remains the same width. The PMO does seem to increase for a better visual system.

5.2.3   VMS , GFD and IFD

When comparing all three simulators for the conditions with a stimulus frequency of 5 rad/s, only one metric was significantly different across simulators: the CZ upper thresholds. Based on the thresholds calculated from the measured signals, the post-hoc tests showed that statistically, the upper thresholds in the VMS and the IFD were not different from each other but were significantly different from the values in the GFD.

The differences found between the upper thresholds in the VMS and IFD as compared to the GFD are somewhat non intuitive. Similarities could be expected between simulators that have similar visual systems, such as the VMS and the GFD, or simulators with the same motion base, such as the GFD and IFD. In this respect, the GFD could be expected to be in between the VMS and the IFD. The GFD has a newer motion platform than the VMS, with improved performance, but it has a visual system that is not as sophisticated as the one in the IFD.

When comparing the upper thresholds based on the commanded signals, indeed the results fit the expectations, with the VMS showing the

lowest thresholds and the IFD the highest. As noted before, calculating the thresholds from commanded signals might not be entirely correct but does help in understanding how the turnaround bump might influence the subjects' judgment of motion. The lower values for the upper thresholds in the VMS are in agreement with the hypothesis that subjects tuned the motion down to compensate for the turnaround bump.

The comparison of the three simulators might be summarized in a very generic way by saying that better simulators allow for larger differences between the inertial and visual cues. That is, for higher quality systems, subjects are more lenient in their judgment of matching visual and inertial cues. Moving from the VMS to the IFD, the quality of the inertial motion feedback and the visual systems could be said to improve. This improvement led to higher upper thresholds, with the exception of the thresholds in the VMS that include the peaks caused by the turnaround bump. The values obtained for the OZ were not statistically different across simulators but they do show a trend of higher PMO values with increasing simulator quality.

It should be noted that since all subjects performed the experiments in each of the simulators in the same order, an effect of learning should not be disregarded. However, there is some evidence that in this type of task, the effect of learning is negligible. In this experiment, as well as in all experiments described in Valente Pais [38], each condition was always repeated by the same subject two or three times. In Chapter 7 of this reference it is mentioned that the effect of the repetition has never been found. Moreover, in Valente Pais *et al.* [34], three experiments are described where two of these experiments were performed by the same subjects with a few weeks of time in between. Also here, no effect of learning or habituation was found.

5.3   Perception metrics and motion simulation

This study showed that the inertial amplitudes inside the coherence zone are not perceived equally. In fact, the lower inertial amplitudes of the coherence zone seemed to be perceived as the best match for the tested visual amplitudes. This might indicate not only that the use of lower inertial amplitudes is acceptable in flight simulation but that they are in fact, optimal.

If these results were to be used in motion filter tuning, the motion gain (i.e., the ratio between the inertial and visual motion), should generally be less than one, especially for the highest amplitude. This supports the findings of other studies [6, 27–29, 35] where a motion gain of one was judged as too strong. One reason why the one-to-one motion may be judged too strong in a simulation environment may be the quality of the visual display [6, 29]. The increasing PMO values for increasing quality of the visual system, as obtained in the comparison between the GFD and the IFD, seems to support this hypothesis.

Visual amplitude in a simulator environment is perceived differently than in the real world. For example, Kemeny and Panerai [50] showed that in driving simulators, observers underestimate driving speed when image contrast, luminance or texture are reduced. They also observed that drivers underestimate distances to a lead vehicle when compared to a similar situation in a real road.

Therefore, instead of matching the inertial amplitude with the expected displacement in the real world, the inertial amplitude should be matched to the displacement perceived from the virtual world. Current self-motion perception models do not make a distinction whether the motion was felt in the aircraft or in the simulator. Therefore, when minimizing the error between the motion perceived in the aircraft from that perceived in the simulator, both perception models have the same structure and parameters. However in this experiment, the preferred inertial amplitude was lower than the visual amplitude, which might indicate that one-to-one motion was perceived as too strong.

By acknowledging this inertial overestimation and measuring its limits, using either a coherence or an optimal zone or both, one could calculate perception model parameters specific for simulation scenarios.

6 Conclusions

Perception coherence zones (CZ) and optimal zones (OZ) for lateral acceleration were measured in three different simulators for two different visual stimulus amplitudes and two stimulus frequencies.

The OZ was contained within the CZ. The points of mean optimal zone (PMOs) were significantly lower than the points of mean coherence (PMCs) and the OZ excluded only the higher inertial amplitudes within the CZ. Apparently, even though all amplitudes within the CZ are perceived as coherent, some motion amplitudes are preferred over others within that zone. The point of mean coherence (PMC) was significantly higher than the point of mean optimal (PMO) zone. This could be an indication that the optimal amplitude zone is a result of tuning for comfort.

The PMO and the PMC both increased with the visual stimulus amplitude and decreased with the visual stimulus frequency. The coherence zone width (CZW) was affected by the visual amplitude and frequency, with higher amplitudes leading to wider zones and higher frequencies leading to narrower zones. The optimal zone width (OZW) was unaffected by these two independent variables.

Differences in simulator configuration resulted in differences in the measured upper thresholds of the CZ. When considering thresholds determined from the commanded signals, the upper thresholds increased as going from the VMS, to the GFD and then to the IFD. When the thresholds were determined from the measured signals, the VMS showed

the highest upper thresholds because these include large amplitude peaks caused by a "turnaround bump".

The increase in upper thresholds was thought to be related to an increase in overall simulator quality. The values obtained for the OZ were not statistically different across simulators but they do show a trend of higher PMO values with increasing simulator quality.

7   Recommendations

To further investigate the potential of coherence zones (CZ) and optimal zones (OZ) as perceptual metrics to quantify differences in simulator and motion cueing performances, more degrees of freedom, amplitudes and frequencies should be tested across different simulators. One practical way of bypassing the complicated logistics of running multiple simulator studies is to use one simulator and artificially degrade both the motion base performance and the visual system quality (see Nieuwenhuizen [51]).

Further research should also be done to investigate if the constant optimal zone width (OZW) results found for the tested amplitudes also occur at higher amplitudes, and whether comfort has in fact an effect on the optimal zone measurements.

For a better understanding of the differences between the OZ and the CZ the effect of these initial conditions on the zones should be further investigated. In this study, the OZ measurement always started with initial inertial amplitudes that were higher or lower than the visual amplitudes whereas the CZ measurements had an initial inertial amplitude that was close to the amplitude of the visual stimulus. As stated previously, these different initial conditions could have biased the differences found between the two zones. To test this hypothesis the coherence and optimal zones could be measured in the same experimental trial. Subjects could then indicate optimal amplitude first and thereafter the boundaries of the coherence zone, or the other way around.

For applications in motion simulation, it is also important to determine what the impact on behavior is when moving out of the optimal zone while remaining within the coherence zone.

Appendices

References

1. Roark, M.; and Junker, A.: The Effects of Closed Loop Tracking on a Subjective Tilt Threshold in the Roll Axis. *14th Manual Control Proceedings*, 1978, pp. 443 – 450.

2. Hosman, R. J. A. W.; and van der Vaart, J. C.: Vestibular Models and Thresholds of Motion Perception. Results of Tests in a Flight

Simulator. Internal Report LR-265, Delft University of Technology, Faculty of Aerospace Engineering, 1978.

3. Hosman, R. J. A. W.; and van der Vaart, J. C.: Thresholds of Motion Perception and Parameters of Vestibular Models Obtained from Tests in a Motion Simulator. , Delft University of Technology, Delft, The Netherlands, 1980.

4. Samji, A.; and Reid, L. D.: The Detection of Low-Amplitude Yawing Motion Transients in a Flight Simulator. *IEEE Transactions on Systems, Man, and Cybernetics*, vol. 22, no. 2, March/April 1992, pp. 300–306.

5. Zaichik, L. E.; Rodchenko, V.; Rufov, I. V.; Yashin, Y. P.; and White, A. D.: Acceleration Perception. *AIAA Modeling and Simulation Technologies Conference and Exhibit, Portland, OR, USA, August 9-11*, no. AIAA-99-4334, 1999, pp. 512–520.

6. Groen, E. L.; Valenti Clari, M. S. V.; and Hosman, R. J. A. W.: Evaluation of Perceived Motion During a Simulated Takeoff Run. *Journal of Aircraft*, vol. 38, no. 4, July-August 2001.

7. Bos, J. E.; Hosman, R. J. A. W.; and Bles, W.: Visual-vestibular interactions and spatial (dis)orientation in flight and flight simulation. TM-02-C009, TNO Defense, Security and Safety, Soesterberg, The Netherlands, 2002.

8. Greenberg, J.; Artz, B.; and Cathey, L.: The Effect of Lateral Motion Cues During Simulated Driving. *Driving Simulation Conference North America, Dearborn, MI, USA, October 8-10*, 2003.

9. Groen, E. L.; and Bles, W.: How to Use Body Tilt for the Simulation of Linear Self Motion. *Journal of Vestibular Research*, vol. 14, no. 5, 2004, pp. 375–385.

10. Heerspink, H. M.; Berkouwer, W. R.; Stroosma, O.; van Paassen, M. M.; Mulder, M.; and Mulder, J. A.: Evaluation of Vestibular Thresholds for Motion Detection in the SIMONA Research Simulator. *AIAA Modeling and Simulation Technologies Conference and Exhibit, San Francisco, CA, USA, August 15-18*, no. AIAA-05-6502, 2005.

11. Fortmüller, T.; and Meywerk, M.: The Influence of Yaw Movements on the Rating of the Subjective Impression of Driving. *Driving Simulation Conference North America, Orlando, FL, USA*, November 2005.

12. Grant, P. R.; Yam, B.; Hosman, R. J. A. W.; and Schroeder, J. A.: Effect of Simulator Motion on Pilot Behavior and Perception. *Journal of Aircraft*, vol. 43, no. 6, 2006, pp. 1914–1924.

13. Naseri, A.; and Grant, P. R.: Difference Thresholds: Measurement and Modeling. *Proceedings of the AIAA Modeling and Simulation Technologies Conference, Portland, Oregon, Aug. 8-11*, no. AIAA-2011-6245, 2011.

14. Shirley, R. S.; and Young, L. R.: Motion Cues in Man-Vehicle Control – Effects of Roll-Motion Cues on Human Operator's Behavior in Compensatory Systems with Disturbance Inputs. *IEEE Transactions on Man-Machine Systems*, vol. 9, no. 4, Dec. 1968, pp. 121–128.

15. Jex, H. R.; Magdaleno, R. E.; and Junker, A. M.: Roll Tracking Effects of G-Vector Tilt and Various Types of Motion Washout. *Fourteenth Annual Conference on Manual Control*, 1978, pp. 463–502.

16. Greig, G. L.: Masking of Motion Cues by Random Motion: Comparison of Human Performance with a Signal Detection Model. 313, UTIAS, 1988.

17. Grant, P. R.; Yam, B.; Hosman, R. J. A. W.; and Schroeder, J. A.: The Effect of Simulator Motion on Pilot's Control Behavior for Helicopter Yaw Control Tasks. *Proceedings of the AIAA Modeling and Simulation Technologies Conference and Exhibit, San Francisco, CA, USA*, no. AIAA-2005-6304, 2005.

18. Pool, D. M.; Zaal, P. M. T.; van Paassen, M. M.; and Mulder, M.: Effects of Heave Washout Settings in Aircraft Pitch Disturbance Rejection. *Journal of Guidance, Control, and Dynamics*, vol. 33, no. 1, 2010, pp. 29–41.

19. Pool, D. M.; Damveld, H. J.; van Paassen, M. M.; and Mulder, M.: Tuning Models of Pilot Tracking Behavior for a Specific Simulator Motion Cueing Setting. *Proceedings of the AIAA Modeling and Simulation Technologies Conference, Portland, Oregon, Aug. 8-11*, no. AIAA-2011-6322, 2011.

20. Mudd, S.: Assessment of the Fidelity of Dynamic Flight Simulators. *Human Factors: The Journal of the Human Factors and Ergonomics Society*, vol. 10, no. 4, 1968, pp. 351–358. Doi:10.1177/001872086801000405.

21. Schroeder, J. A.: Evaluation of Simulation Motion Fidelity Criteria in the Vertical and Directional Axes. *Journal of the American Helicopter Society*, vol. 41, no. 2, 1996, pp. 44–57.

22. White, A. D.; and Rodchenko, V. V.: Motion Fidelity Criteria Based on Human Perception and Performance. *AIAA Modeling and Simulation Technologies Conference and Exhibit, Portland, OR, USA, August 9-11*, no. AIAA-1999-4330, 1999, pp. 485–493.

23. Schroeder, J. A.: Helicopter Flight Simulation Motion Platform Requirements. NASA/TP-1999-208766, NASA, Moffet Field, CA, July 1999.

24. Hosman, R.; and van der Vaart, J.: Effects of Vestibular and Visual Motion Perception on Task Performance. *Acta Psychologica*, vol. 48, no. 1-3, 1981, pp. 271 – 287.

25. Harris, L. R.; Jenkin, M.; and Zikovitz, D. C.: Visual and Non-visual Cues in the Perception of Linear Self Motion. *Exp Brain Res*, vol. 135, no. 1, 2000, pp. 12–21.

26. Grant, P.; and Lee, P. T. S.: Motion-Visual Phase-Error Detection in a Flight Simulator. *Journal of Aircraft*, vol. 44, no. 3, 2007, pp. 927–935.

27. Feenstra, P.; Wentink, M.; Correia Grácio, B. J.; and Bles, W.: Effect of Simulator Motion Space on Realism in the Desdemona Simulator. *DSC 2009 Europe*, Monaco, 2009.

28. Pretto, P.; Nusseck, H. G.; Teufel, H. J.; and Bülthoff, H. H.: Effect of Lateral Motion on Driver's Performance in the MPI Motion Simulator. *DSC 2009 Europe*, Monaco, 2009.

29. Groen, E. L.; Smaili, M. H.; and Hosman, R. J. A. W.: Perception Model Analysis of Flight Simulator Motion for a Decrab Maneuver. *Journal of Aircraft*, vol. 44, no. 2, 2007, pp. 427 – 435.

30. Grant, P. R.; and Haycock, B.: Effect of Jerk and Acceleration on the Perception of Motion Strength. *Journal of Aircraft*, vol. 45, no. 4, 2008, pp. 1190 – 1197.

31. van der Steen, F. A. M.: An Earth-Stationary Perceived Visual Scene During Roll and Yaw Motions in a Flight Simulator. *Journal of Vestibular Research*, vol. 8, no. 6, 1998, pp. 411–425.

32. van der Steen, F. A. M.: Self-Motion Perception. Ph.D. Thesis, Delft University of Technology, 1998.

33. Valente Pais, A. R.; van Paassen, M. M.; Mulder, M.; and Wentink, M.: Perception of Combined Visual and Inertial Low-Frequency Yaw Motion. *AIAA Modeling and Simulation Technologies Conference, Toronto, ON, Canada, August 2-5*, no. AIAA 2010-8093, 2010, pp. 1–10.

34. Valente Pais, A. R.; van Paassen, M. M.; Mulder, M.; and Wentink, M.: Perception Coherence Zones in Flight Simulation. *Journal of Aircraft*, vol. 47, no. 6, 2010, pp. 2039–2048.

35. Correia Grácio, B. J.; van Paassen, M. M.; Mulder, M.; and Wentink, M.: Tuning of the Lateral Specific Force Gain Based on Human Motion Perception in the Desdemona Simulator. *AIAA Modeling and Simulation Technologies Conference and Exhibit, Toronto, ON, Canada, August 2-5*, no. AIAA-2010-8094, 2010.

36. Valente Pais, A. R.; van Paassen, M. M.; Mulder, M.; and Wentink, M.: Effect of Performing a Boundary-Avoidance Tracking Task on the Perception of Coherence Between Visual and Inertial Cues. *AIAA Modeling and Simulation Technologies Conference, Portland, OR, USA, August 8-11*, no. AIAA 2011-6324, 2011, pp. 1–13.

37. Jonik, P. M.; Valente Pais, A. R.; van Paassen, M. M.; and Mulder, M.: Phase Coherence Zones in Flight Simulation. *AIAA Modeling and Simulation Technologies Conference and Exhibit*, no. AIAA 2011-6555, Portland, OR, August 2011.

38. Valente Pais, A. R.: Perception Coherence Zones in Vehicle Simulation. Ph.D. Thesis, Delft University of Technology, Faculty of Aerospace Engineering, May 2013.

39. Correia Grácio, B. J.; Valente Pais, A. R.; van Paassen, M. M.; Mulder, M.; Kelly, L. C.; and Houck, J. A.: Optimal and Coherence Zone Comparison Within and Between Flight Simulators. *Journal of Aircraft*, vol. 50, no. 2, 2013, pp. 493–507.

40. Fernandez, C.; and Goldberg, J. M.: Physiology of Peripheral Neurons Innervating Otolith Organs of the Squirrel Monkey. III. Response Dynamics. *Journal of Neurophysiology*, vol. 39, no. 5, 1976, pp. 996–1008.

41. Soyka, F.; Robuffo Giordano, P.; Beykirch, K.; and Bülthoff, H. H.: Predicting Direction Detection Thresholds for Arbitrary Translational Acceleration profiles in the Horizontal Plane. *Experimental Brain Research*, vol. 209, no. 1, 2011, pp. 95–107.

42. Grant, P. R.; and Haycock, B.: The Effect of Jerk and Acceleration on the Perception of Motion Strength. *Proceedings of the AIAA Modeling and Simulation Technologies Conference and Exhibit, Keystone, CO, USA*, no. AIAA-2006-6253, 2006.

43. Sinacori, J. B.: The Determination of Some Requirements for a Helicopter Research Simulation Facility. Contractor Report NAS2-9421 NASA-CR-152066, NASA, Ames Research Center, Moffet Field, CA, USA, September 1977.

44. Hosman, R. J. A. W.: Pilot's Perception and Control of Aircraft Motions. Ph.D. Thesis, Delft University of Technology, Faculty of Aerospace Engineering, 1996.

45. Chung, W. W. Y.; Sweet, B. T.; and Lewis, E.: Visual Cueing Effects Investigation for a Hover Task. *AIAA Modeling and Simulation Technologies Conference and Exhibit, Austin, TX, USA, August 11-14*, , no. AIAA-2003-5524, 2003.

46. Brandt, Th.; Dichgans, J.; and Koenig, E.: Differential Effects of Central Versus Peripheral Vision on Egocentric and Exocentric Motion Perception. *Experimental Brain Research*, vol. 16, no. 5, 1973, pp. 476–491. Doi:10.1007/BF00234474.

47. Held, R.; Dichgans, J.; and Bauer, J.: Characteristics of Moving Visual Scenes Influencing Spatial Orientation. *Vision Research*, vol. 15, no. 3, 1975, pp. 357–365. Doi:10.1016/0042-6989(75)90083-8.

48. Kawakita, T.; Kuno, S.; Miyake, Y.; and Watanabe, S.: Body Sway Induced by Depth Linear Vection in Reference to Central and Peripheral Visual Field. *The Japanese Journal of Physiology*, vol. 50, no. 3, 2000, pp. 315–321.

49. Nakamura, S.: The Perception of Self-Motion Induced by Central and Peripheral Visual Stimuli Moving in Opposite Directions. *Japanese Psychological Research*, vol. 43, no. 3, 2001, pp. 113–120. Doi:10.1111/1468-5884.00167.

50. Kemeny, A.; and Panerai, F.: Evaluating Perception in Driving Simulation Experiments. *TRENDS in Cognitive Sciences*, vol. 7, no. 1, 2003, pp. 31–37.

51. Nieuwenhuizen, F. M.: Changes in Pilot Control Behaviour Across Stewart Platform Motion Systems. Ph.D. Thesis, Delft University of Technology, Faculty of Aerospace Engineering, July 2012.

REPORT DOCUMENTATION PAGE

1. REPORT DATE *(DD-MM-YYYY)*	2. REPORT TYPE	3. DATES COVERED *(From - To)*
01-02-2015	Technical Memorandum	

4. TITLE AND SUBTITLE	5a. CONTRACT NUMBER
Comparison of Flight Simulators Based on Human Motion Perception Metrics	5b. GRANT NUMBER
	5c. PROGRAM ELEMENT NUMBER

6. AUTHOR(S)	5d. PROJECT NUMBER
Valente Pais, Ana R.; Correia Gracio, Bruno L.; Kelly, Lon C.; Houck, Jacob A.	5e. TASK NUMBER
	5f. WORK UNIT NUMBER
	160961.01.01.01

7. PERFORMING ORGANIZATION NAME(S) AND ADDRESS(ES)	8. PERFORMING ORGANIZATION REPORT NUMBER
NASA Langley Research Center Hampton, VA 23681-2199	L-20530

9. SPONSORING/MONITORING AGENCY NAME(S) AND ADDRESS(ES)	10. SPONSOR/MONITOR'S ACRONYM(S)
National Aeronautics and Space Administration Washington, DC 20546-0001	NASA
	11. SPONSOR/MONITOR'S REPORT NUMBER(S)
	NASA-TM-2015-218681

12. DISTRIBUTION/AVAILABILITY STATEMENT
Unclassified - Unlimited
Subject Category 54
Availability: NASA STI Program (757) 864-9658

13. SUPPLEMENTARY NOTES

14. ABSTRACT

In flight simulation, motion filters are used to transform aircraft motion into simulator motion. When looking for the best match between visual and inertial amplitude in a simulator, researchers have found that there is a range of inertial amplitudes, rather than a single inertial value, that is perceived by subjects as optimal. This zone, hereafter referred to as the optimal zone, seems to correlate to the perceptual coherence zones measured in flight simulators. However, no studies were found in which these two zones were compared. This study investigates the relation between the optimal and the coherence zone measurements within and between different simulators. Results show that for the sway axis, the optimal zone lies within the lower part of the coherence zone. In addition, it was found that, whereas the width of the coherence zone depends on the visual amplitude and frequency, the width of the optimal zone remains constant.

15. SUBJECT TERMS

Coherence zone; Flight simulators; Motion; Motion perception; Optimal zone; Simulators; Visual

16. SECURITY CLASSIFICATION OF:			17. LIMITATION OF ABSTRACT	18. NUMBER OF PAGES	19a. NAME OF RESPONSIBLE PERSON
a. REPORT	b. ABSTRACT	c. THIS PAGE			STI Help Desk (email: help@sti.nasa.gov)
U	U	U	UU	54	19b. TELEPHONE NUMBER *(Include area code)* (757) 864-59658